Naval Research Laboratory
Washington, DC 20375-5320

NRL/MR/6110--11-9344

# ESTCP UXO Innovation Technology Transfer Project

## ESTCP Project MM-0744
## GEMTADS Demonstration at F.E. Warren AFB
## Demonstration Data Report

N. Khadr
D.A. Keiswetter

*SAIC, Inc. - ASAD*
*Arlington, Virginia*

G.R. Harbaugh
D.A. Steinhurst

*Nova Research, Inc.*
*Alexandria, Virginia*

June 6, 2011

# REPORT DOCUMENTATION PAGE

*Form Approved*
*OMB No. 0704-0188*



**1. REPORT DATE** *(DD-MM-YYYY)*
06-06-2011

**2. REPORT TYPE**
Memorandum Report

**3. DATES COVERED** *(From - To)*
August 2007 – October 2007

**4. TITLE AND SUBTITLE**
ESTCP UXO Innovation Technology Transfer Project
ESTCP Project MM-0744
GEMTADS Demonstration at F.E. Warren AFB
Demonstration Data Report

**5a. CONTRACT NUMBER**

**5b. GRANT NUMBER**

**5c. PROGRAM ELEMENT NUMBER**
0603851D8Z

**5d. PROJECT NUMBER**
MM-0744

**5e. TASK NUMBER**

**5f. WORK UNIT NUMBER**
61-5802-W-0

**6. AUTHOR(S)**
N. Khadr,* D.A. Keiswetter,* G.R. Harbaugh,† and D.A. Steinhurst†

**7. PERFORMING ORGANIZATION NAME(S) AND ADDRESS(ES)**
Naval Research Laboratory, Code 6110
4555 Overlook Avenue, SW
Washington, DC 20375-5320

**8. PERFORMING ORGANIZATION REPORT NUMBER**
NRL/MR/6110--11-9344

**9. SPONSORING / MONITORING AGENCY NAME(S) AND ADDRESS(ES)**
Environmental Security Technology Certification Program (ESTCP) Program Office
901 North Stuart Street, Suite 303
Arlington, VA 22203

**10. SPONSOR / MONITOR'S ACRONYM(S)**
ESTCP

**11. SPONSOR / MONITOR'S REPORT NUMBER(S)**

**12. DISTRIBUTION / AVAILABILITY STATEMENT**
Approved for public release; distribution is unlimited.

**13. SUPPLEMENTARY NOTES**
*SAIC, Inc. - ASAD, 1225 South Clark Street, Suite 800, Arlington, VA 22202
†Nova Research, Inc., 1900 Elkin Street, Suite 230, Alexandria, VA 22308

**14. ABSTRACT**
A geophysical survey of two 9-acre areas within the boundary of the F.E. Warren AFB Closed Base Range MRA was conducted as part of the Environmental Security Technology Certification Program (ESTCP) Unexploded Ordnance (UXO) Innovative Technology Transfer Project. The survey was conducted using the Naval Research Laboratory (NRL) GEMTADS frequency-domain EMI sensor array. The two survey areas were selected from previous data in cooperation with the stakeholders to foster a comparison between the existing geophysical technologies and methodologies being used on site with the GEMTADS platform and a data processing methodology recently demonstrated as part of the ESTCP UXO Discrimination Study as a possible avenue of technology transfer from the research community into the field. This report documents the data collection effort and provides an archive for the collected data sets and other generated data products. In addition, results of the data processing effort to build classifiers based on the available ground truth are presented and the construction of a prioritized dig list are discussed.

**15. SUBJECT TERMS**

| | | |
|---|---|---|
| Discrimination | Multi-sensor Towed Array Detection System (MTADS) | Frequency-Domain EMI |
| Classification | Electromagnetic Induction (EMI) | |
| Unexploded Ordnance (UXO) | GEMTADS | |

| 16. SECURITY CLASSIFICATION OF: a. REPORT | b. ABSTRACT | c. THIS PAGE | 17. LIMITATION OF ABSTRACT | 18. NUMBER OF PAGES |
|---|---|---|---|---|
| Unclassified | Unclassified | Unclassified | UL | 71 |

**19a. NAME OF RESPONSIBLE PERSON**
B.J. Spargo, NRL, Code 6110

**19b. TELEPHONE NUMBER** *(include area code)*
(202) 404-6392

**Standard Form 298 (Rev. 8-98)**
**Prescribed by ANSI Std. Z39.18**

# Contents

# Figures

# Tables

# Abbreviations Used

| **Abbreviation** | **Definition** |
|---|---|
| AFB | Air Force Base |
| AFCEE | U.S. Air Force Center for Engineering and the Environment |
| AMTADS | Airborne Multi-sensor Towed Array Detection System |
| CD-R | Compact Disk - Recordable |
| COG | course-over-ground |
| DAQ | Data Acquisition (System) |
| DAS | Data Analysis System |
| DVD-R | Writable digital versatile disc |
| EM(I) | ElectroMagnetic Induction |
| ESTCP | Environmental Security Technology Certification Program |
| FA | False Alarm |
| FAR | False Alarm Rate |
| FEW | F.E. Warren AFB |
| FQ | Fix Quality |
| GEMTADS | MTADS GEM-3 sensor array |
| GPO | Geophysical Prove-Out (area) |
| GPS | Global Positioning System |
| HASP | Health and Safety Plan |
| Hz | Hertz |
| IDA | Institute for Defense Analyses |
| IMU | Inertial Measurement Unit |
| MC | Munitions Constituents |
| MEC | Munitions and Explosives of Concern |
| MM | Munitions Management |
| MRA | Munitions Response Area |
| MRS | Munitions Response Site |
| MTADS | Multi-sensor Towed Array Detection System |
| MX | "Missle-X" or Peacekeeper missle system. The missle is officially designated as a LGM-118A |
| NAD83 | North American Datum of 1983 |
| NAVD88 | North American Vertical Datum of 1988 |
| NMEA | National Marine Electronics Association |
| NRL | Naval Research Laboratory |
| nT | nanoTesla |
| Pd | Probability of Detection |
| POC | Point of Contact |
| PP | Peak-to-Peak |
| (PTNL,)AVR | Time, Yaw, Tilt, Range for Moving Baseline RTK NMEA-0183 message |
| (PTNL,)GGK | Time, Position, Position Type, DOP NMEA-0183 message |

# Abbreviations Used (cont.)

| Abbreviation | Definition |
|---|---|
| QA | Quality Assurance |
| QAO | Quality Assurance Officer |
| QAPP | Quality Assurance Project Plan |
| QC | Quality Control |
| RI | Remedial Investigation |
| ROC | Receiver Operating Characteristic |
| RTK | Real Time Kinematic |
| SHERP | Safety, Health, and Emergency Response Plan |
| SNR | Signal to Noise Ratio |
| SSO | Site Safety Officer |
| SUXOS | Senior UXO Supervisor |
| TBD | To Be Determined |
| UTC | Universal Coordinated Time |
| UXO | Unexploded Ordnance |
| VHF | Very High Frequency |
| WAA | Wide Area Assessment |
| WGS 84 | World Geodetic System 1984 |
| ZIP (250) | Iomega ZIP disk (250 MB version) |

## ACKNOWLEDGEMENTS

Glenn Harbaugh and Daniel Steinhurst (P.I.) of Nova Research, Inc., and Nagi Khadr of SAIC, Inc. (ASAD) comprised the field team responsible for the data collection. Nagi Khadr and Dean Keiswetter (SAIC – ASAD) conducted the analysis of the results presented in this report. This work was supported by ESTCP under project MM-0744.

The P.I. would like to thank F.E. Warren AFB, especially John Wright, Chief of Environmental Restoration for F.E. Warren AFB for making this demonstration possible. Brian Powers and Andy Gascho of URS Corporation, Inc. assisted in the planning of this demonstration. Joe Goehring of URS provided invaluable assistance with site logistics and our field operations at F.E. Warren AFB.

## ABSTRACT

Nova Research conducted a geophysical survey of two 9-acre areas within the boundary of the F.E. Warren AFB (FEW) Closed Base Range MRA as part of the Environmental Security Technology Certification Program (ESTCP) Unexploded Ordnance (UXO) Innovative Technology Transfer Project. The survey was conducted using the Naval Research Laboratory (NRL) GEMTADS frequency-domain EMI sensor array. URS Corporation, Inc. has been previously tasked by the U.S. Air Force Center for Engineering and the Environment (AFCEE) to conduct a Remedial Investigation (RI) of munitions, explosives of concern (MEC), and munitions constituents (MC) within the Munitions Response Area (MRA). The two survey areas were selected in cooperation with the stakeholders to foster a comparison between the existing geophysical technologies and methodologies being used in the RI with the GEMTADS platform and a data processing methodology recently demonstrated as part of the ESTCP UXO Discrimination Study as a possible avenue of technology transfer from the research community into the field. The WWI and WWII vintage ranges within the MRA include mostly 37-mm and 75-mm projectile and small arms ranges. This demonstration data report serves to document the data collection results of this demonstration and to provide an archive for the collected data sets and other generated data products. In addition, results of the data processing effort to build classifiers based on the available ground truth are presented and the feasibility of their immediate use for discrimination and the construction of a prioritized dig list are discussed.

# ESTCP UXO Innovative Technology Transfer Project

# GEMTADS Demonstration at F.E. Warren AFB

### Cheyenne, WY

### September, 2007

## 1. Introduction

### 1.1 Background

In FY 2007, the Environmental Security Technology Certification Program (ESTCP) was directed by the United States Congress to establish an Unexploded Ordnance (UXO) Innovative Technology Transfer Project. The project was directed to conduct evaluations of innovative UXO technologies at military munitions response sites (MRSs) in coordination with remediation project managers. In December 2006, ESTCP solicited nominations for sites interested in hosting one of the technology demonstrations. Over twenty nominations were received.

The ESTCP Program Office selected three sites for participation in this year's efforts: Ft. McClellan in Anniston, AL; F.E. Warren AFB outside Cheyenne, WY; and the Blossom Point Research Facility, Welcome, MD. At each of the sites, the technologies to be demonstrated in the ESTCP UXO Innovative Technology Transfer Project were chosen to complement and extend ongoing efforts at the site. The technologies scheduled for demonstrations range from cued discrimination using EMI sensors to underwater ordnance detection using magnetometer arrays.

#### 1.1.1 Specific Objective of Demonstration

URS Corporation, Inc. has been tasked by the U.S. Air Force Center for Engineering and the Environment (AFCEE) to conduct a Remedial Investigation (RI) of munitions, explosives of concern (MEC), and munitions constituents (MC) on the Closed Base Ranges at F.E. Warren Air Force Base (AFB), Wyoming (FEW), an active installation outside Cheyenne, WY. The WWI and WII vintage ranges include mostly 37-mm and 75-mm projectiles and small arms ranges. Since 2003, the RI has consisted of transect and comprehensive geophysical surveys using Geonics EM61 MkII sensors as well as localized surface sweeps and intrusive investigation of targets.

As part of the ESTCP UXO Innovative Technology Transfer Project, Nova Research, Inc. conducted a geophysical survey of approximately 19 acres of the Closed Base Ranges using the U.S. Naval Research Laboratory (NRL) Multi-sensor Towed Array Detection System (MTADS) GEM-3 (GEMTADS) sensor array as a possible technology transfer candidate to support the

---

Manuscript approved May 3, 2011.

ongoing RI. The data were collected in accordance with the overall Project goals and the requests of the stakeholders.

# 2. Technology Description

## 2.1 Technology Development and Application

The demonstration was conducted using the NRL MTADS. The MTADS has been developed with support from ESTCP. The MTADS hardware consists of a low-magnetic-signature vehicle that is used to tow several different sensor arrays over large areas (10 - 25 acres / day) to detect buried UXO. The MTADS tow vehicle and the GEMTADS array are shown in Figure 2-1. Positioning is provided using cm-level Real Time Kinematic (RTK) Global Positioning System (GPS) receivers. The positioning technology requires the availability of one or more known first-order survey control points to use as reference stations.

Figure 2-1 – MTADS GEM-3 (GEMTADS) array in survey configuration with the MTADS tow vehicle

### 2.1.1 GEM-3 (GEMTADS) Array

The GEM-3 sensor is a frequency-domain EMI sensor developed by Geophex, Ltd. The MTADS GEMTADS array consists of three, 96-cm diameter GEM-3 sensors in a triangular configuration with two sensors across the front of the array and one centered in the rear. The nominal ride height of the sensors is 33.5 cm above the ground. Figure 2-1 show the configured array being pulled by the MTADS tow vehicle. The roughly 2-m square array is shown schematically in Figure 2-2. Figure 2-3 is a close-up photograph of the array with the sensors false-colored (sensor #1 shown in red, sensor #2 in green, and sensor #3 in blue). This color scheme is used throughout the remainder of the document and in the DAQ software displays. The array is mounted on a rigid support which is attached to the MTADS EMI trailer using non-metallic fasteners. A plastic tarp can be added to improve thermal stability and as protection from precipitation, when required.

Individual sensors in the array are located using a three-receiver RTK GPS system shown schematically in Figure 2-2 [1]. The three-receiver configuration extends the concept of RTK operations from that of a fixed base station and a moving rover to moving base stations and moving rovers. The lead GPS receiver (MB1) receives corrections from the fixed base station at 1 Hz. This corrected position is reported at 10-20 Hz using a vendor-specific National Marine Electronics Association (NMEA) NMEA-0183 message format (PTNL, GGK, or GGK). The MB1 receiver also operates as a ‘moving base,’ transmitting corrections (by serial cable) to the next GPS receiver (MB2) which uses the corrections to operate in RTK mode.  A vector (AVR1, heading (yaw), angle (pitch), and range) between the two antennae is reported at 10 Hz using a vendor-specific NMEA-0183 message format (PTNL, AVR, or AVR).  MB2 also provides 'moving base' corrections to the third GPS receiver (MR) and a second vector (AVR2) is reported at 10 Hz.  All GPS measurements are recorded at full RTK precision, ~2-5 cm.  All sensor readings are referenced to the GPS 1-PPS output to fully take advantage of the precision of the GPS measurements.

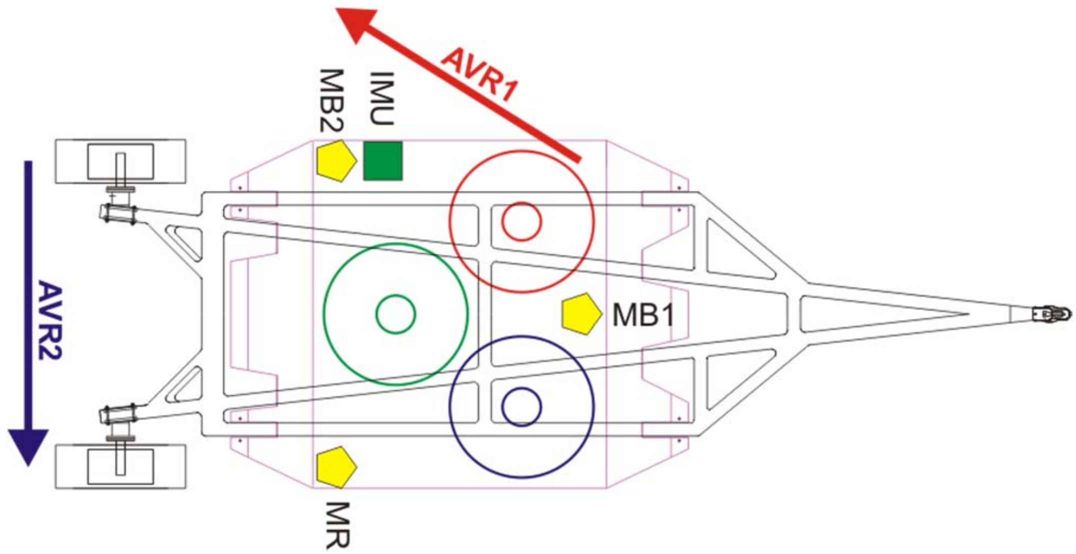


Figure 2-2 – MTADS EM trailer with approximate locations of GPS and IMU equipment indicated.  The colored circles represent the GEM-3 sensors of the GEMTADS array.

Figure 2-3 – MTADS GEM-3 array mounted on the EM sensor trailer.  In addition to the three GEM-3 sensors, note the three GPS antennae and the IMU for platform motion measurement.  The sensors are false-colored as discussed in the text.  The IMU is the small black box mounted under the MB2 GPS antenna.

An Inertial Measurement Unit (IMU) is also included on the sensor array to provide complementary platform orientation information. The IMU is a Crossbow VG300 running at 30 Hz. The physical position of the IMU is shown in Figure 2-3.

The standard GEM-3 sensor drive electronics have been modified to produce a substantially higher transmit moment for this array. Each individual sensor can transmit a composite waveform of one to ten frequencies in the frequency range of 30 to 20,010 Hz with a base period of 1/30 sec. For this survey, a composite transmitter waveform of nine frequencies log-spaced from 90 to 20,010 Hz was used. All demonstrations to date of the GEMTADS array have used this composite waveform. Two additional base periods are required for signal deconvolution and to output the response from each sensor. The array can therefore operate continuously with one sensor actively transmitting while the other two sensors are processing data at any given time. Allowing for a short coil settling time between the transmissions from each sensor, an effective array sampling rate of just over 9 Hz is achieved. Sequential transmitter operation also alleviates the need for the orthogonal survey mode employed for the EM61 MkII array. Coupled with our standard survey speed of 3 mph, the result is a down-track sampling spacing of ~15 cm. The cross-track spacing is 50 cm. An interleaved survey pattern is used to decrease the cross-track spacing to 25 cm as depicted in Figure 2-4. In some cases, such as at survey area corners with limited availability of area outside the site to turn the system around (e.g. a fence line), the orthogonal survey pattern used for the MTADS EM61 MkII has proven more efficient and is functionally equivalent.

The GEM-3 sensors are controlled by a custom electronics package designed and built by Geophex, Ltd. It is mounted in an equipment rack in the MTADS tow vehicle as shown in Figure 2-5. Overall control of data collection is accomplished with a custom version of the standard GEM-3 sensor control software, WinGem2KArr, running under Windows 2000 on our data acquisition computer. An example of the working screen of this program is shown in Figure 2-6. This software package logs the data from the GEM-3 sensors, the three GPS NMEA sentences, the time of the GPS 1-PPS pulse, the GPS UTC time stamp, and the IMU data in separate files with a common base survey name. The IMU is software triggered at 30 Hz by a custom software application written at NRL. The data are periodically transferred to the data analyst for immediate QC checks and for further processing. Refer to Appendix B, Section B.9 for the details of the file formats.

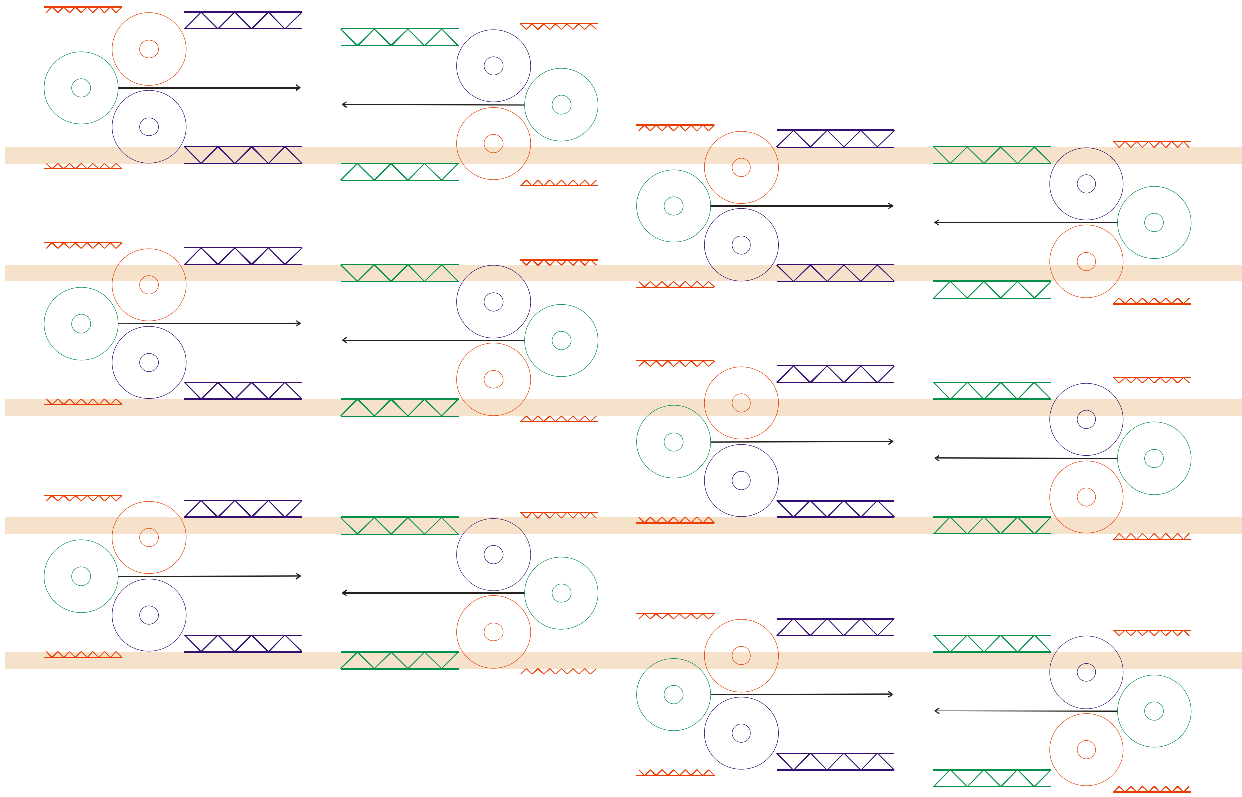

Figure 2-4 – Schematic of the interleaved survey pattern for GEMTADS surveys. The sensors are depicted as colored circles. The large cross-hatched sections indicate the path of the tow vehicle tires. The outer extents of the swath of the EM trailer tires are represented by the narrow cross-hatching. The tan bars represent areas where two tire tracks are collocated.


Figure 2-5 – GEM-3 array control electronics and GPS receivers rack-mounted in the MTADS tow vehicle

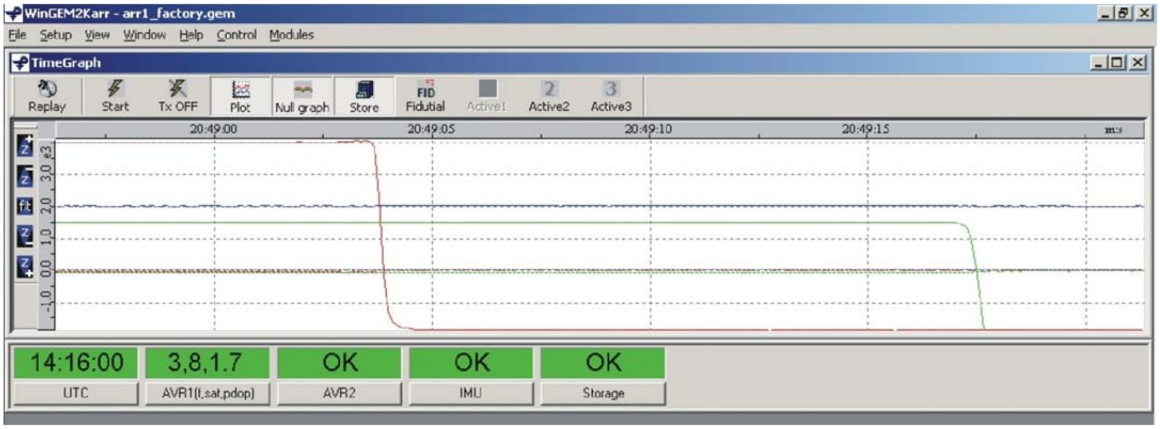


Figure 2-6 – Working screen of the WinGEM2kArr program

### 2.1.2 Pilot Guidance System

The GPS positioning information used for data collection is shared with an onboard navigation guidance display and provides real-time navigational information to the operator. The guidance display was originally developed for the airborne adjunct of the MTADS system (AMTADS) [2] and is installed in the vehicle and available for the operator to use. Figure 2-7 shows a screenshot of the guidance display configured for vehicular use.

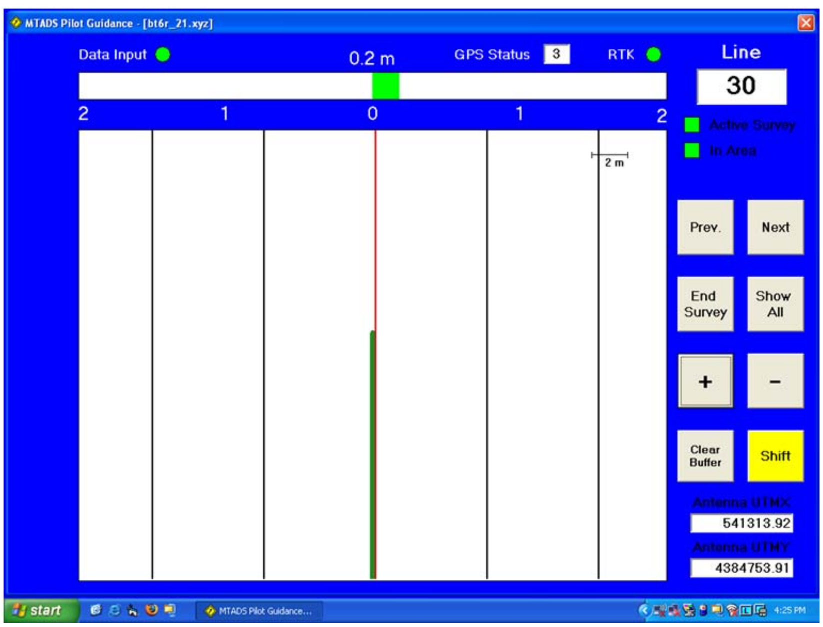


Figure 2-7 – Screenshot of MTADS Pilot Guidance application display

An integral part of the guidance display is the ability to import a series of planned survey lines (or transects) and to guide the operator to follow these transects. In the context of this demonstration, the pilot guidance display can be used to guide the operator to the survey area and provide immediate feedback on progress and data coverage. The display provides a left-right course correction indicator, an optional altitude indicator for aircraft applications, and color-coded flight swath overlays where the current transect is displayed in red and the other transects are displayed in black for operator reference. The survey course-over-ground (COG) is plotted for the operator in real time on the display. The COG plot is color-coded based on the RTK GPS system status. When fully operational, the COG plot is color-coded green. If the system status is degraded, the COG plot color changes from green to yellow to red (based on severity) to warn the operator and allow for on-the-fly reacquisition of the affected area. Figure 2-7 shows the operator surveying line 30 of a transect plan.

### 2.1.3 Data Analysis Methodology

#### 2.1.3.1 Data Collection QC Workflow

Each data set is collected using the WinGem2KArr software package. The collected raw data are preprocessed on site for quality assurance purposes using standard MTADS procedures and checks. The data set is comprised of eight separate files, each containing the data from a single system device. See Appendix B, Section B.9 for further details about file contents and formats. Each device has a unique data rate. During the data import phase of the QC process, software written by SAIC computes the average data rate for each file as the file is being processed. Any discrepancies are flagged for the Data Analyst to address. After the data import and QC phase, the data are transferred to Oasis montaj to locate and map the data. As part of the import process any data corresponding to a sensor outage, a GPS outage, or a vehicle stop / reverse, are defaulted or marked to not be processed further. Defaulted data are not deleted and can be recovered at a later time if so desired. An example of the working screen for examining the GPS data is shown in Figure 2-8. Any long wavelength features such as sensor drift and large scale geology are filtered from the data (demedianed). In the montaj environment, the data sets are subjected to further QC analysis by the Data Analyst and then assembled into complete site / survey area databases. An example montaj working screen is shown in Figure 2-9.

#### 2.1.3.2 Anomaly Detection and Detection Threshold Selection

Anomalies are extracted from the composite site databases in a manner similar to that used for the ESTCP UXO Discrimination Study demonstration at Former Camp Sibert [7]. Any anomaly with a peak magnitude greater than the determined threshold is identified and placed on the anomaly pick list. The process of selecting an appropriate threshold requires information about the item(s) of interest, the response of the sensor to the item(s) of interest, and the goals of the demonstration especially in terms of the depth of interest. The detection threshold is selected based on the predicted peak anomaly magnitude for the item of interest. As the items of interest could be positioned in a range of orientations and at a range of depths, response curves are generated bounding the sensor response at the most favorable orientation and at the least favorable orientation of the sensor / item of interest pair with respect to the exciting field and as a function of depth.

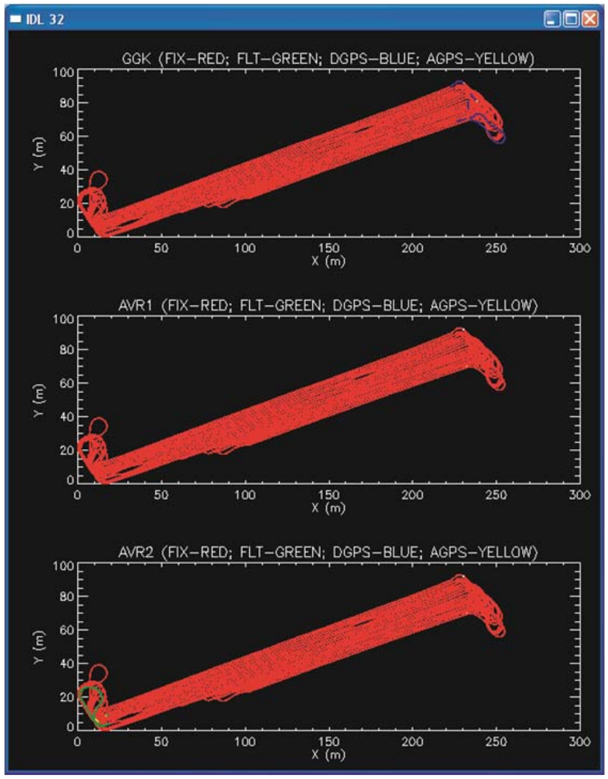


Figure 2-8 – Screenshot of the GPS monitoring tool

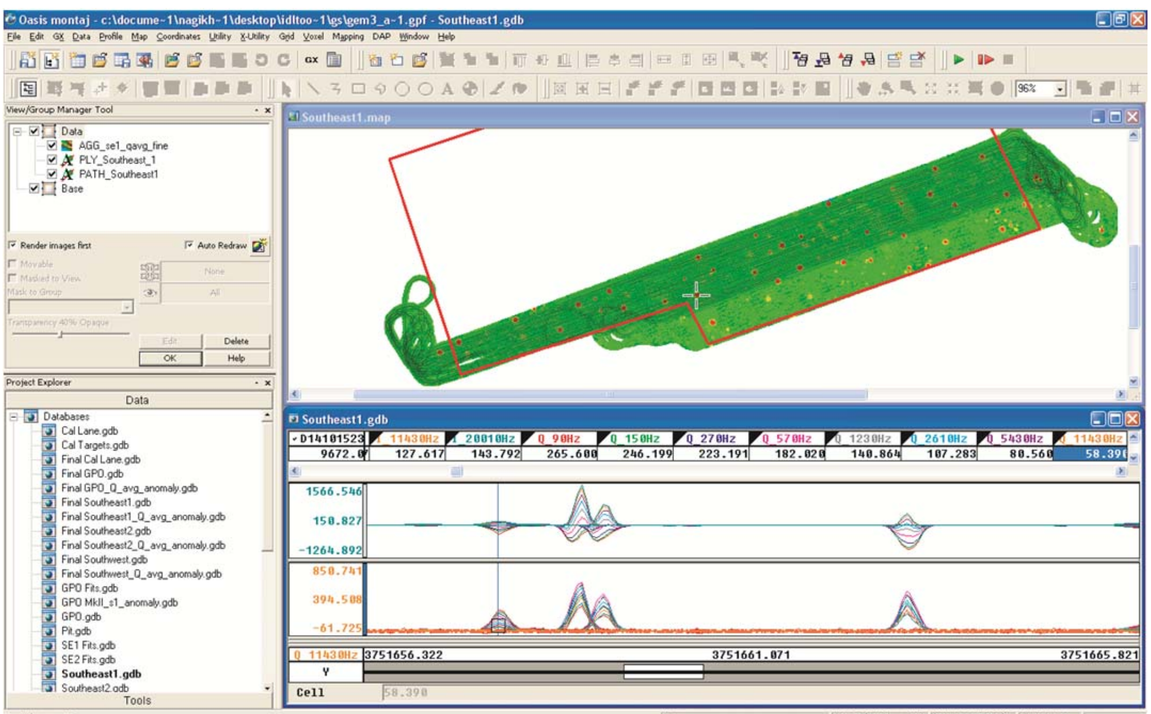


Figure 2-9 – Screenshot of the data processing working screen in Oasis montaj

An example is given in Figure 2-10 for the GEMTADS system and a 4.2-in mortar (107 mm diameter), the item of interest from the Former Camp Sibert demonstration. For the GEMTADS array, the quadrature-based metric $Q_{ave}$ has been found to be effective for anomaly detection.

$$Q_{ave} = \frac{\sum (Q_{270Hz} + Q_{570Hz} + Q_{1230Hz} + Q_{2610Hz} + Q_{5430Hz})}{5}$$

The upper curve represents the sensor response (in ppm, $Q_{ave}$) for the most favorable orientation of the projectile with respect to the exciting field (the GEM-3 transmitter) as a function of depth below the surface. The sensors travel an additional 33.5 cm above the surface. The lower curve represents the sensor response for the least favorable orientation. The results of pit measurements made under field conditions on site are shown as black circles. A representative noise level from a nearby GPO is also shown. For this example, the demonstration design set the initial depth of interest to be 11x the diameter of the item of interest, or 1.17 m for the 4.2-in mortar. At this depth, the initial threshold was set to be one-half the least-favorable predicted response, or 1.3 ppm, $Q_{ave}$ in this example where the least favorable response is predicted to be 2.6 ppm, $Q_{ave}$. This safety factor of two was requested by the ESTCP UXO Discrimination Study stakeholders.

As part of the ongoing RI at the Closed Base Ranges at FEW, there is an available geophysical prove-out area (GPO) on site containing many of the munitions types that have been found in the MRA included 37-mm and 75-mm projectiles. To date, the 37-mm and 75-mm projectiles have proven to be the bulk of the munitions recovered during the RI and will be the primary focus of this demonstration.

The munitions were buried at a variety of depths and orientations to determine the site-specific detection thresholds and detection depths for the various items. Data were collected with the GEMTADS array over this GPO to establish the appropriate anomaly detection threshold for this site and items of interest. The data processing and the results are discussed in Section 3.2.6.

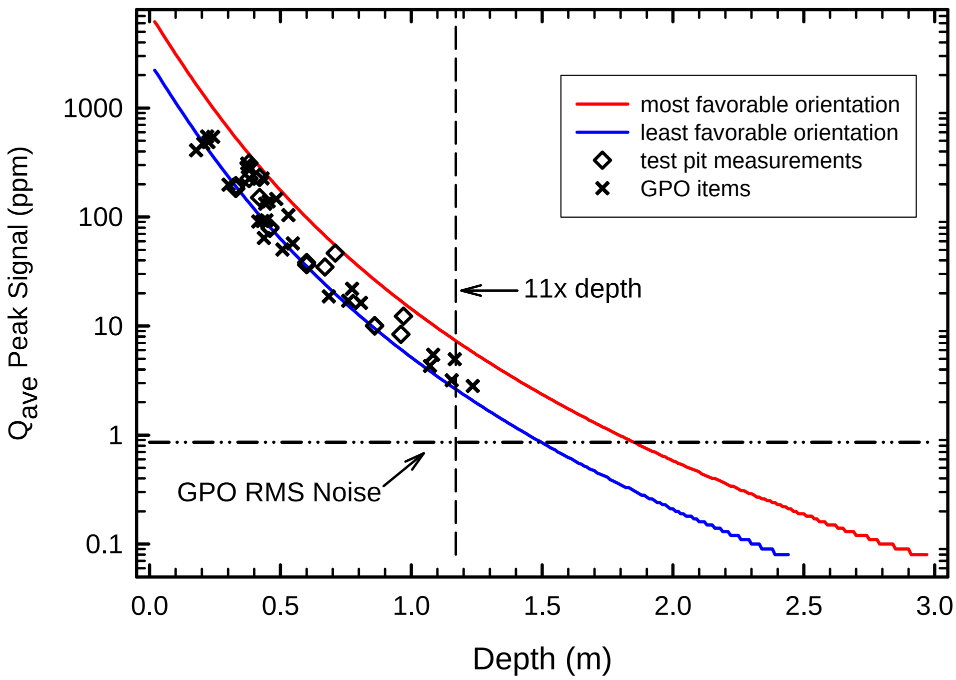


Figure 2-10 – Peak anomaly amplitude results from the GEMTADS and pit measurements of the 4.2-in mortar (open diamonds). The modeled system response for the most (red) and least (blue) favorable orientations of the mortar are shown as lines. The responses for the seeded GPO items are also shown as 'x's.

#### 2.1.3.3 Classifier and Discrimination Data Processing Workflow

The located demedianed GEMTADS data (position, orientation, and 9 data pairs (in-phase and quadrature response for 9 transmit frequencies)) surrounding the center of each selected anomaly are extracted and submitted to the solver engine developed by SAIC, Inc. for the analysis of the GEMTADS data collected at Camp Sibert as part of the ESTCP UXO Discrimination Project. Inversion of GEMTADS data is done using a standard dipole model. The solver algorithm finds 6 fitted parameters: $x, y, z, \phi, \theta, \psi$, where $x, y, z$, are the target coordinates (m) and $\phi, \theta, \psi$, are the Euler angles (deg) of the model output. The associated best-fit betas (three, $\beta$), chi-squared ($\chi^2$), and coherence are also found as part of the inversion. The betas are the principal components of the induced magnetization tensor. The $\chi^2$ and coherence are measures of the quality of the inversion result with respect to the original source data. Follow-on fits are made while constraining the three βs to match appropriate given values from a library containing values for items including the items of interest. The associated $\chi^2$ and coherence values are found for the fit to each library item, and the ratios of (constrained coherence) / (un-constrained coherence) are calculated for each fit.

To prevent the solver from becoming trapped in local minima, the unconstrained inversion process operates in two stages. The first stage steps through fixed $z$ values from the ground surface down to a maximum depth of 1.75m. At each $z$ step, the best-fit target $x,y$ position is found using the "matrix" method in which elements of the response tensor are found through linear regression. This method permits fast run times and experience has shown that it is robust against local minima. No restrictions are placed on the tensor values: they may be positive or negative, even for quadrature data which are normally only positive. Each channel is treated independently, so each will have a different apparent target orientation.

The ten best solutions, judged by $\chi^2$ value, are used as starting points in the second unconstrained inversion stage. Prior to submitting these data, the Euler angles must be determined. Previous work has shown that using arbitrary angle values for the initial conditions can lead to failure of the solver due to local minima. Therefore, a special optimization step is performed separately on each of the ten best solutions. In this step, "best-fit" Euler angles are found through minimization of off-diagonal elements in the response tensor, across all channels. The starting points for this optimization are the apparent Euler angles from each channel's tensor. The second unconstrained inversion stage searches all 6 fitted parameter values: $x, y, z, \phi, \theta, \psi$, through a downhill simplex minimization. After cycling through all ten of the start points from the first inversion stage, the best-ever solution is saved.

It has been found that making an adjustment to the in-phase data improved performance, based on available ground truth. The adjustment consists of removing the local mean from the In-phase data at each measurement point: At each point, the mean in-phase value across all channels is found and subtracted from all in-phase data at that point. A parameter search is then performed, and finally, best-fit βs are determined through regression on the full, unadjusted data set.

For each anomaly processed in the described manner, all fitted results are reported; including position ($x,y,z$), orientation (three angles), polarizability spectra, $\chi^2$ error, the correlation coefficient between model and measured data, and a signal strength metric. Both unconstrained and library-constrained inversions are performed, assuming that representative spectra are observed for certain classes of objects (such as the UXO targets of interest or unique clutter classes). The size of an equivalent sphere is also estimated from the βs via established parametric models.

Once the inversions of all anomalies are complete, the resultant fit parameters, or features, are examined to identify those which are appropriate for building the classifier for the discrimination process and generating the prioritized dig list. The available features are examined to find those features which cluster the anomalies into discrete groupings either as a function of a single feature or as a distance from a central position in a feature plane. At this point in the process, a site-specific set of training data with available ground truth is used to identify those features and clusters that correspond to the items of interest and those that correspond to other items such as clutter. Using the best identified classifier and thresholds, the anomalies are then ranked in a prioritized dig list. The prioritized dig list is similar in nature to the ones provided for the UXO Discrimination Study where the anomalies are ranked into five categories: (1) high confidence clutter (don't dig), (2) moderate/low confidence clutter (dig), (3) can not analyze (dig), (4) moderate/low confidence UXO (dig), and (5) high confidence UXO (dig). The prioritized dig list is then provided in the form of an Excel spreadsheet.

An example from the ongoing analysis of the GEMTADS data collected at the Former Camp Sibert is shown in Figure 2-11 [3]. The 4.2-in mortar was the item of interest at this site. Figure 2-11 shows a plot of the coherence ratio (constrained fit / unconstrained fit) versus signal strength, $Q_{sum}$, were $Q_{sum}$ is defined as the sum of all quadrature frequency responses for the anomalies in the provided training data. The coherence ratio and $Q_{sum}$ represent a possible set of features for building a classifier. A decision line (similar to a 1D threshold) is generated and an example is shown in the Figure as a solid line. In this example, items with a response below 200 ppm, $Q_{sum}$ would be classified as 'can not invert, dig' as the coherence ratio becomes a less valuable classification tool at these low signal levels. The remaining items are then classified based on the distance from the decision line being used as a measure of the confidence of the classification. Those items that are below and furthest from the line would be declared 'high-confidence non-targets of interest." Those items above the line would be declared UXO with the confidence of that classification again scaled by the distance from the decision line. In this case, those items with a coherence ratio of 0.95 or higher would be declared 'high-confidence target of interest." To determine the dig-no dig threshold, a ROC curve would be generated and the distance from the decision line that correctly classifies all UXO (i.e. $P_d$ of 1.0) including a safety margin would be determined. This distance would then be the threshold for the dig-no dig decision.

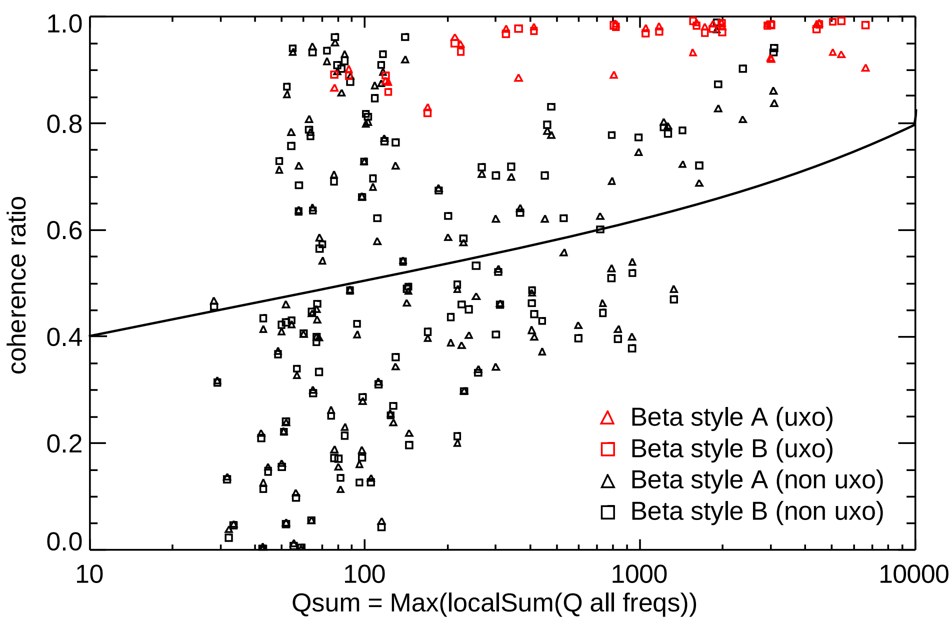


Figure 2-11 – An example of GEMTADS fit results for the training set data from Former Camp Sibert

The data processing workflow outlined above requires that a validated set of training data be available upon completion of the individual anomaly analysis portion of the data processing work flow. These training data are used to identify the relevant features and clustering of the anomalies. The only training data available are the GPO data. Examination of the GPO ground truth provided by URS shows that there are no non-munitions related items, or clutter emplaced in the GPO.

## 2.2 Previous Testing of the Technology

The Chemistry Division of the Naval Research Laboratory has participated in several programs funded by SERDP and ESTCP whose goal has been to enhance the discrimination ability of

MTADS for both the magnetometer and EM-61 array configurations. The process has been based on making use of both the location information inherent in an item's magnetometry response and the shape and size information inherent in the response to the time-domain electromagnetic induction (EMI) sensors that are part of the baseline MTADS in either a cooperative or joint inversion. In all these efforts, our classification ability has been limited by the information available from the EMI sensor. The EM61 is a time-domain instrument with either a single gate to sample the amplitude of the decaying signal (MkI) or four gates relatively early in time (MkII). The first generation of the MTADS EM61 MkII array was demonstrated in 2001 [4] at the Badlands Bombing Range, SD with little demonstrable gain over the single decay of the MkI array. A second generation of the MkII array with updated electronics was constructed in 2003.

To make further progress on UXO discrimination, a sensor with more available information was required. The Geophex, Ltd. GEM-3 sensor is a frequency-domain sensor with up to ten transmit frequencies available for simultaneous measurement of the in-phase and quadrature response of the target. In principle, there will therefore be much more information available from a GEM-3 sensor for use in discrimination decisions. However, the commercial GEM-3 sensor is a hand-held instrument with relatively slow data rates and is thus not very amenable to rapid, wide area surveys.

ESTCP Project MM-0033, Enhanced UXO Discrimination Using Frequency-Domain Electromagnetic Induction, was funded to overcome this limitation by integrating an array of GEM-3 sensors with the MTADS platform [5]. The project objective was to demonstrate the optimum system built around the Geophex GEM-3 EMI sensor that delivers the most discrimination performance while retaining acceptable survey efficiency. A three-sensor array system was designed around a modified GEM-3 sensor. The system was built and characterized in 2002 and 2003 and then demonstrated at the Standardized UXO Demonstration sites at Aberdeen Proving Ground and Yuma Proving Ground in 2003 and 2004. At each of the sites, the Calibration Lanes, the Blind Test Grid, and as much of the Open Field Area as was possible were surveyed. For the Blind Test Grid and the Open Field, the ranked target picks were submitted to the Aberdeen Test Center for scoring. Appendix A summarizes the performance of the GEMTADS array at both sites as reported in Reference 5. Reference 6 compares the detection-only performance of both the second-generation MTADS EM61 MkII and the GEMTADS arrays to other demonstrators at both of the Standardized UXO Technology Demonstration Sites. The MTADS EM61 MkII and GEMTADS arrays were demonstrated in the Spring of 2007 as part of the ESTCP UXO Discrimination Study at the Former Camp Sibert [7]. Data processing and the development of performance results for the various discrimination methodologies of the UXO Discrimination Study are discussed in ESTCP Pilot Program Classification Approaches in Munitions Response Final Report [8].

### 2.3 Advantages and Limitations of the Technology

On large open ranges the vehicular MTADS provides an efficient survey technology. Surveys with the magnetometer array often exceed production rates of 20 acres per day. Production rates for the EM systems range from one-half to one-quarter that of the magnetometer system to maintain sufficiently high data densities. UXO items with gauges larger than 20mm are typically detected to their likely burial depths. The detection performance of MTADS magnetometer, EM61 MkII, and GEMTADS arrays for the range of munitions types and sizes emplaced at the Standardized UXO Demonstration sites are documented in References 6 and 7 and the references within.

In the past, a human operator has manually selected the data corresponding to individual anomalies. With the experience gained as part of the WAA Pilot Project and the UXO Discrimination Study, robust automated anomaly extraction methodologies have been developed to significantly reduce the operational burden on the human operator. Using a site-specific anomaly extraction threshold for the item(s) of interest which takes into account any stakeholder guidance, an automated routine can extract the location of all anomalies above the threshold in an unbiased manner with no operator involvement.

The located, demedianed GEMTADS data (position, orientation, and 9 data pairs (In-phase and Quadrature response for 9 transmit frequencies)) surrounding the center of each selected anomaly are then extracted and submitted to the solver engine developed by SAIC, Inc. for the analysis of the GEMTADS data collected at Camp Sibert as part of the ESTCP UXO Discrimination Project. Inversion of GEMTADS data is done using a standard dipole model. The solver algorithm finds 6 fitted parameters: $x, y, z, \phi, \theta, \psi$, where $x, y, z$, are the target coordinates (m) and $\phi, \theta, \psi$, are the Euler angles (deg) of the model output. The associated best-fit betas (three, $\beta$), chi-squared ($\chi^2$), and coherence are also found as part of the inversion. Therefore, the operator efforts are focused on the development of the feature-based classifiers used to build the prioritized dig list based on stakeholder requirements and experience, rather than on the mechanics of anomaly detection and data processing.

The presence of certain terrain features such as deep ravines without good crossing points, thick clusters of trees, and other non-navigable features such as steep hill faces can limit the areas that can be surveyed. The presence of long barbed-wire fences without gates and deep ravines, steep hill and plateau faces without good access points can also slow survey operations by reducing survey line length and increasing travel time to traverse these obstacles.

# 3. Demonstration Design

## 3.1 Performance Objectives

Performance objectives for the demonstration are given in Table 3-1 to provide a basis for evaluating the performance and costs of the demonstrated technology. These objectives are for the technologies being demonstrated only. Overall project objectives will be given in the overall demonstration plan generated by ESTCP. The final column, 'Actual Performance Objective Met?' will be added in future reports.

Table 3-1 – Performance Objectives/Metrics and Confirmation Methods

| Type of Performance Objective | Performance Criteria | Expected Performance (Metric) | Performance Confirmation Method |
|---|---|---|---|
| **Qualitative** | *Reliability and Robustness* | *General Observations* | *Operator feedback and recording of system downtime (length and cause)* |
| **Quantitative** | | | |
| | | **Data Collection** | |
| | *Survey Rate* | *5 acres / day* | *Calculated from survey results* |
| | *Data Density* | *> 20 pts / m*$^2$ | *Calculated from survey results* |
| | *Percentage of Assigned Coverage Completed* | *100% as allowed by topography / vegetation* | *Calculated from survey results* |
| | *On-site Data Throughput* | *All data QC'ed in real time and data preparation for analysis completed on site* | *Analysis of records kept / log files generated while in the field and recorded completion times* |
| | | **Data Analysis** | |
| | *Anomaly Detection Threshold* | *GPO survey data establishes a detection threshold which is sufficiently above the site background level to detect the items of interest to the depth of interest* | *Analysis of GPO data and generation of response curves for 37-mm and 75-mm projectiles and comparison to existing data on depth distribution of items of interest* |
| | *Data Quality of Inversion Results* | *Data from anomalies with low fit errors (<50%) can be successfully inverted and classified* | *Comparison of signal strength for emplaced GPO items, inversion results (fit error), and classification (ID) with no clutter training data* |

## 3.2 Testing and Evaluation Plan

### 3.2.1 Demonstration Set-Up and Start-Up

F.E. Warren AFB (FEW) has served a number of functions since its activation as a military base in the mid-1800s. A brief history of the munitions usage and MEC concerns for the Closed Base Ranges at F.E. Warren AFB can be found in Reference 9, and is summarized here. U.S. Army outpost Fort D.A. Russell was established at the same location in 1867. In 1930, the base was renamed for Francis E. Warren, the Wyoming senator who played an important role in the development of the post. During World War II, the size of the installation more than doubled to support new missions, including the training of Army personnel. In 1947, the base was transferred to the newly formed Air Force, under control of the Air Training Command. The Strategic Air Command assumed jurisdiction over the installation in 1958. FEW was the first base selected for deployment of Atlas D missiles, and became the operations center for the Atlas intercontinental ballistic missile in 1960. In 1965, the Atlas missiles were replaced by 200 Minuteman I missiles. Minuteman III missiles replaced Minuteman I missiles in 1975. FEW was assigned to the Air Combat Command in June 1992, and then to the Air Force Space Command in July 1993. At present, the primary mission of FEW is to provide operational, maintenance, and security support for 150 Minuteman III missiles and for the deactivation of the Peacekeeper (MX) missile system.

An archive data collection effort was performed at FEW from 23–26 June 2003 to determine the status of past and current range activities, as well as to collect relevant environmental and operational data on the range areas identified [10]. This data collection effort resulted in the generation of several historic range maps for FEW. A number of small arms and artillery ranges were identified from historical records and are noted in Reference 9. Two active ranges were identified within the Closed Bases Ranges perimeter and one adjacent to the area, the Explosives Ordnance Disposal (EOD), the Small Arms Firing Range, and the Trap Range. These areas remain active and are excluded from the RI activities.

FEW and AFCEE contracted URS Corporation, Inc. to conduct an RI of the Closed Base Ranges beginning in 2003 to identify and further delineate the MRSs within the munitions response area (MRA). The data are being used to evaluate the MRSs for further response subsequent to the RI activities.

As part of the ESTCP UXO Innovative Technology Transfer Project, Nova Research, Inc. conducted a geophysical survey of approximately 19 acres within the FEW Closed Base Ranges MRA using the NRL GEMTADS sensor array. The MTADS vehicular system was mobilized to the demonstration site in a U.S. Navy-owned 53-ft trailer by a government-contracted transportation company. The 53-ft trailer transported the tow vehicle, the sensors and sensor trailer, notebook computers for the analysis team, GPS equipment, batteries and chargers, office equipment, radios and chargers, tools, equipment spares, and maintenance items to the site.

Some essential support services were available on-site. Accordingly, Nova Research made arrangements to acquire the remaining necessary supplies, materials, and facilities from appropriate local vendors.

A 9’ x 48’ shipping container, which could be fully opened at one end for drive-in access, was mobilized to the site to garage and for secure storage of the MTADS vehicle and sensor platform. The 48’ shipping container and the 53’ trailer were placed in between the two survey areas on a field road for all-around easy access. Power to the trailers was provided by a field generator (8 kW) provided by URS. NRL’s standby 4 kW generator was available for use but was not required. The power was used to recharge the vehicle batteries overnight. Communications among on-site personnel was provided by hand-held VHF radios provided to all field personnel. The VHF radio and GPS batteries were charged overnight in the URS office trailer and picked up each morning on the way out to the site. Cellular phone service on site was good throughout the site and also used for communications. Communications with the URS teams operating on site was maintained with a single radio from one of the FEW radio networks provided by URS. A portable toilet was mobilized to support the field crew during the field effort.

FEW is located directly west of Interstate 25 outside Cheyenne, WY. The demonstration site is located in the middle to northern portions of the MRA. Three potential 8.25-acre (600 ft x 600 ft) survey areas were identified by URS and prioritized in terms of value to ongoing efforts and to the various stakeholders. The prioritization is indicated in the area labels (Priority Area 1 is the first priority) and the approximate corner coordinates for the areas are given in Table 3-2. Figure 3-1 shows the MRA site boundary and the prioritized survey areas. Priority Areas 1 and 2 were surveyed during this demonstration. Priority Area 3, held in reserve to cover any emergent issues while the team was in the field, was not used. The main criteria for selecting these areas were: a) a target anomaly density of 100-200 anomalies/acre and b) to generate useful comparison data between methods currently being considered at FEW for remediation and the GEMTADS to foster a potential technology transfer scenario. Existing results for the RI were used to estimate the anomaly densities. A Priority Area 4 is shown in Figure 3-1 but was not part of this demonstration.

Upon arrival, the team personnel established the base camp and set up for field operations. There are eight GPS control points available within the MRA. The details are listed in Table 3-3. The coordinates of the provided geodetic control points are given in Table 3-3 (horizontal datum: World Geodetic System (WGS 84); vertical datum: NAVD88). The RTK GPS base station receiver and radio link was established on CATM 99-1, one of the available established control points. CATM 99-1 was chosen to provide good coverage of the GPO and both survey areas and for its easy access from the access road to the survey areas. The validity of the control point location was verified by the Quality Assurance Officer (QAO) using a man-portable RTK GPS rover receiver to occupy the control points CATM 99-3, Delta, and Fox. Control point CATM 99-1, occupied by the GPS base station, served as the reference for this test.

The measured locations of the three tested control points were found to be within 2-3 cm of their reported locations, verifying the internal consistency of the control point network. A discrepancy discovered with the locations of the GPO seed items is discussed in Section 3.2.5. A USACE control point located on a concrete pier was found near Priority Area 1 and the position was recorded for future QC efforts. The monument marker ID field is blank and an elevation (6,291.45 ft) is stamped on the marker. The RTK-measured coordinates are given in Table 3-3.

The EM trailer with the GEM-3 sensors was connected to the tow vehicle and the system was powered up after being unloaded from the 53’ trailer. The connectivity of the sensors to the DAQ computer and the establishment of normal SNR performance were verified along with the operational state of the vehicle RTK system. Details of the standard MTADS calibration diagnostic procedures are given in Section 3.2.10. These data were collected and submitted to the Data Analyst for evaluation. These data were also collected every field day in accordance with the procedures outlined in Section 3.2.10.

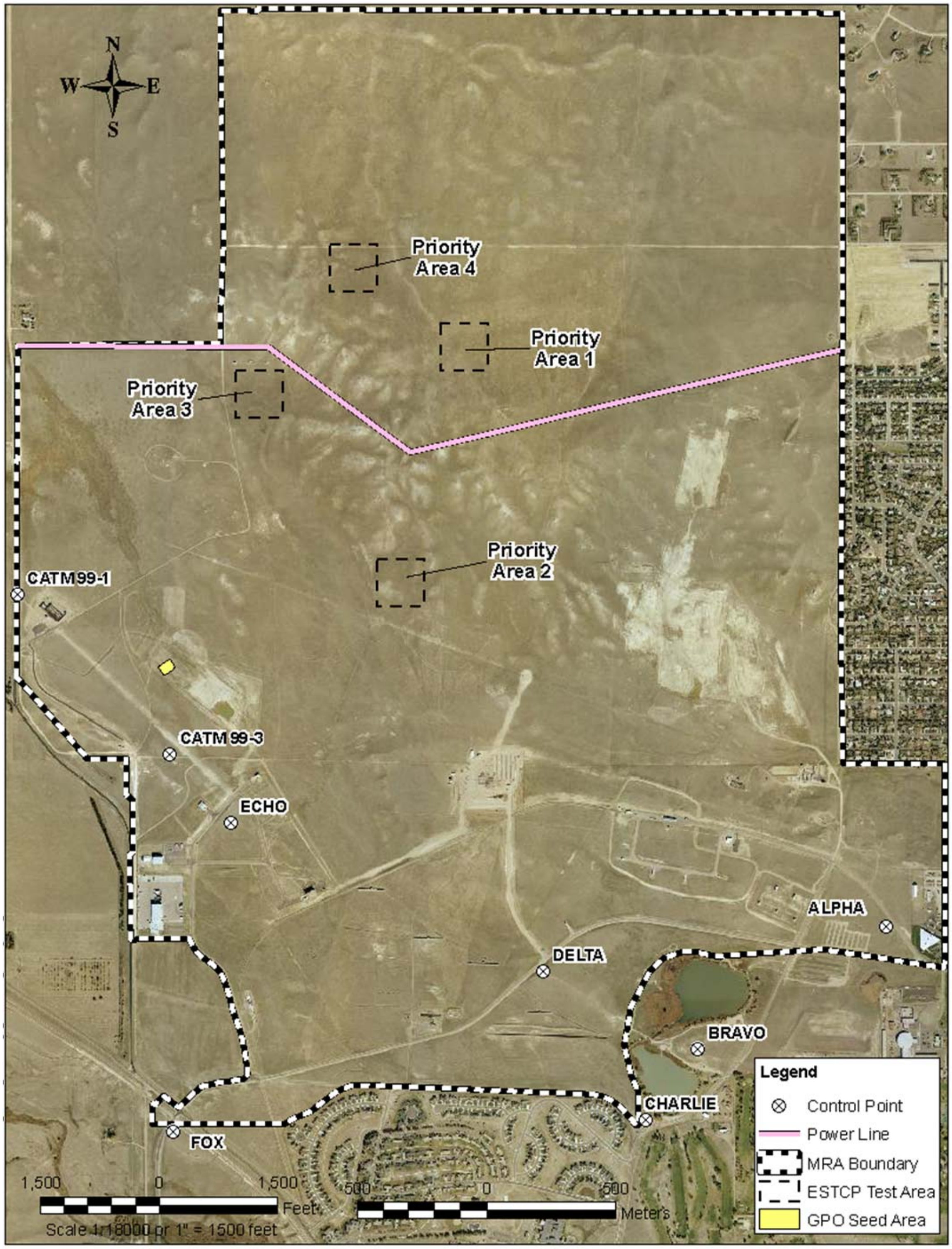


Figure 3-1 – Available survey areas within the F.E. Warren AFB Closed Base Ranges MRA. The survey areas are labeled by stakeholder priority. Figure provided by URS.

Table 3-2 – Proposed survey area boundaries for the demonstration

| Survey Area / Corner ID | Easting (m) | Northing (m) | Survey Area / Corner ID | Easting (m) | Northing (m) |
|---|---|---|---|---|---|
| | UTM 13N, WGS 84 | | | UTM 13N, WGS 84 | |
| Priority Area 1 NW | 511,213.526 | 4,559,893.210 | Priority Area 3 NW | 510,786.806 | 4,560,198.010 |
| Priority Area 1 NE | 511,396.406 | 4,559,893.210 | Priority Area 3 NE | 510,969.686 | 4,560,198.010 |
| Priority Area 1 SE | 511,396.406 | 4,559,710.330 | Priority Area 3 SE | 510,969.686 | 4,560,015.130 |
| Priority Area 1 SW | 511,213.526 | 4,559,710.330 | Priority Area 3 SW | 510,786.806 | 4,560,015.130 |
| Priority Area 2 NW | 510,969.686 | 4,558,978.810 | | | |
| Priority Area 2 NE | 511,152.566 | 4,558,978.810 | | | |
| Priority Area 2 SE | 511,152.566 | 4,558,795.930 | | | |
| Priority Area 2 SW | 510,969.686 | 4,558,795.930 | | | |

Table 3-3 – Available Survey Control Points at F.E. Warren AFB

| Point | Latitude | Longitude | HAE (m) | Elevation (m)* | Northing (m) | Easting (m) |
|---|---|---|---|---|---|---|
| | WGS 84 | | | NAVD88 | UTM Zone 13N, WGS 84 | |
| CATM 99-1 | 41º 10’ 51.07547” N | 104º 53’ 08.93029” W | 1,881.994 | 1,897.759 | 4,558,840.204 | 509,576.923 |
| CATM 99-3 | 41º 10’ 30.99830” N | 104º 52’ 43.70502” W | 1,888.076 | 1,903.888 | 4,558,221.881 | 510,165.473 |
| ALPHA | 41º 10’ 09.28039” N | 104º 50’ 44.66056” W | 1,872.626 | 1,888.624 | 4,557,556.557 | 512,940.342 |
| BRAVO | 41º 09’ 53.96697” N | 104º 51’ 15.91398” W | 1,870.574 | 1,886.533 | 4,557,083.084 | 512,212.875 |
| CHARLIE | 41º 09’ 45.01244” N | 104º 51’ 24.59328” W | 1,862.149 | 1,878.099 | 4,556,806.619 | 512,011.073 |
| DELTA | 41º 10’ 03.70733” N | 104º 51’ 41.62125” W | 1,872.238 | 1,888.154 | 4,557,382.469 | 511,613.335 |
| ECHO | 41º 10’ 22.40499” N | 104º 52’ 33.65434” W | 1,876.405 | 1,892.236 | 4,557,957.219 | 510,400.027 |
| FOX | 41º 09’ 43.77514” N | 104º 52’ 43.18168” W | 1,871.925 | 1,887.758 | 4,556,765.683 | 510,179.697 |
| Unnamed USACE CP | 41º 11’ 24.97426” N | 104º 52’ 00.77172” W | 1,902.470 | 1,918.322 | 4,559,887.797 | 511,163.253 |

* Provided elevations were used to generate HAE measurements using the NAVD88/Geoid03 vertical datum for all points except the USACE point. For the USACE point, the measured HAE value (referenced to CATM 99-1) was used to generate the elevation using the NAVD88/Geoid03 vertical datum.

The URS SUXOS and Site Safety Officer (SSO) provided a brief orientation to the site for the field team the first morning on site. The project SSO conduct a ‘tail-gate’ safety meeting each day that field personnel were on site. The topic(s) for each day’s meeting were at the discretion of the project SSO.

Preventative maintenance inspections were conducted at least once a day by all team members, focusing particularly on the tow vehicle and the sensor trailer. Any identified deficiencies were addressed according to the severity of the deficiency. Parts, tools, and materials for many maintenance scenarios were available in the system spares inventory which was located on site.

### 3.2.2 Period of Operation

A tentative schedule for the major items in the Demonstration is given in tabular form in Table 3-4. All times associated with survey activities are now finalized with the completion of field work. See Section 3.2.3 for a discussion of the post-field work activities.

Table 3-4 – GEMTADS F.E. Warren AFB Demonstration Planning Schedule

| **Date** | **Planned Action** |
|---|---|
| Week of August 27th | Pack equipment and load the 53 ft. trailer at Blossom Point, MD. |
| Tue, September 4th | 53 ft. trailer picked up at Blossom Point, MD for transit. |
| Fri, September 7th | URS personnel received and positioned the 53' trailer, first shipping container, and portable toilet. |
| Sun, September 9th | Personnel arrived in Cheyenne, WY. Unpacked 53' trailer and assembled / tested MTADS GEMTADS system. |
| Mon, September 10th | Surveyed GPO. Began survey of Priority Area 1. |
| Tue, September 11th | Completed survey of Priority Area 1. Began survey of Priority Area 2. |
| Wed, September 12th | Completed survey of Priority Area 2. Packed 53 ft. trailer. |
| Thu, September 13th | Trailer departed for Blossom Point, MD. Personnel depart site. |
| Mon, September 17th | Trailer arrived at Blossom Point, MD. |
| Week of October 22nd | Submit Draft Demonstration Data Report to ESTCP. |

### 3.2.3 Scope of Demonstration

Data collection was conducted at the ESTCP UXO Innovative Technology Transfer Project Demonstration Site at F.E. Warren AFB at the request of the ESTCP Program Office. The site is located within the F.E. Warren AFB Closed Base Ranges, outside Cheyenne, WY. The demonstration site is composed of two areas with a total acreage of approximately 19 acres. Total coverage surveys were conducted using the NRL MTADS GEM-3 (GEMTADS) array. These data were collected in accordance with the overall Project goals and the requests of the stakeholders. Located, preprocessed data for each area are delivered as a site database archive with this report. A site-specific anomaly detection threshold was determined for the two items of interest identified by the stakeholders for the site, the 37-mm and the 75-mm projectile. This threshold was based on data collected from the onsite GPO. For each site database, all anomalies above the selected threshold were identified and an anomaly list generated. A subset area of approximately 4.5 acres was selected within Priority Area 1 that contained approximately 1,400 anomalies for individual anomaly analysis and for data collection by other data collection demonstrators involved in the project. The selection of the subset area was made in cooperation with the Program Office after completion of the field work. This document, the Demonstration Data Report, was submitted to document the anomaly detection threshold selection, the individual anomaly analysis results, and a proposed classifier and discrimination scheme.

This Demonstration Data Report includes the analysis of the individual anomalies within the selected subset and a discussion of the features identified for building potential classifiers based on thresholds and clustering. A recommendation is presented for a classifier-based discrimination of the anomalies within the selected subset. The available training data are limited to the GPO which contains no clutter items, limiting our ability to definitively characterize the performance of the proposed classifier scheme.

### 3.2.4 Operational Parameters for the Technology

The main operational parameters in this study are the determination of the appropriate site and item-of-interest specific anomaly detection threshold for the GEMTADS sensor array, the identification of the features used to generate the discrimination classifier, and the scheme for ordering the anomaly analysis results into a prioritized dig list based on this classifier. Data collected on the available GPO was used to establish the anomaly extraction threshold. See Section 3.2.6 for the discussion of how the anomaly detection threshold was selected. Additionally, the GPO data set was used to fine tune the solver used for the inversion process, including the development / refinement of library elements (βs) for the 37-mm and 75-mm projectiles to be used for the library-constrained inversions. See Section 2.1.3 for a discussion of the discrimination process. Based on the inversion results and the GPO results, a classifier was built from the available data features. The classifier and a numerical classification scheme was then used to generate prioritized dig lists with a ranking of (1) high confidence clutter (don't dig), (2) moderate/low confidence clutter (dig), (3) can not analyze (dig), (4) moderate/low confidence UXO (dig), and (5) high confidence UXO (dig).

### 3.2.5 Geophysical Prove Out (GPO)

A geophysical prove out area (GPO) was previously emplaced on site near the two survey areas. The emplaced items are munitions that are of the types recovered on site during previous remediation efforts including the primary Items of Interest, the 37-mm and 75-mm projectiles. A few recovered items were also emplaced, such as a Stokes mortar. The items were emplaced at a range of depths and orientations to explore the maximum detection depth of the items, including some at depths that are likely beyond detection using current technologies. Using an EM61 MkII sensor (Geonics, Ltd.), URS has established a range of anomaly detection thresholds for the MkII sensor and the munitions and MC found on site under actual site conditions. Using these anomaly detection thresholds, depths of detection and $P_d$ / FAR statistics were determined for the sensor / Items of Interest / site combination [9]. We surveyed the GPO with the GEMTADS array to collect data to aid in establishing the anomaly detection threshold used for this GEMTADS demonstration. URS has provided the ground truth for the GPO to us to aid in our analysis. To extract the most information possible from the GPO, we surveyed the GPO in two orthogonal directions using the interleaved survey pattern for each direction. This was important because the GPO results are all of the ground truth information that is available for developing classifiers for discrimination. The survey data and ground truth from the GPO were used by the data processors to develop library elements (βs) for the 37-mm and 75-mm projectiles and to fine-tune the solver developed for the ESTCP UXO Discrimination Study at Former Camp Sibert for the site conditions and the Items of Interest prior to beginning the main data processing effort.

A discrepancy was found between the apparent locations of the emplaced GPO items and the reported locations for the items. When we surveyed the GPO, we found that the apparent locations of the GPO items were shifted slightly from the reported positions. URS records indicate that the emplaced items were located using RTK GPS but with an unknown reference base station point. URS now exclusively uses satellite-augmented GPS (sub-meter) for data collection. As a result, we shifted the reported GPO item locations using the apparent offset prior to analyzing our GPO data. The Berkeley group that was also collecting data at FEW as part of this project was apprised of the discrepancy. Until the nature of the offset is better understood, we recommend that any further efforts use control point CATM 99-1 for the reference base station to ensure co-registration of data sets. The offsets are given in Table 3-5.

Table 3-5 – Offsets for GPO emplaced items

| **UTM 13N, WGS 84** | |
|---|---|
| Δ(Easting) | -2.219 m |
| Δ(Northing) | -0.813 m |

The GPO data sets are included on the attached CD. Figure 3-2 presents an anomaly map (ppm, $Q_{ave}$) for the GPO when surveyed in a Northwest to SouthEast direction. Figure 3-3 is the same anomaly map with the emplaced items encircled by polygons and labeled by ID. Note that there are also several, large-amplitude anomalies indicated that do not correspond to emplaced items. Figure 3-4 presents an anomaly map (ppm, $Q_{ave}$) for the GPO when surveyed in a Northeast to Southwest direction. When comparing Figure 3-2 and Figure 3-4, there is clearly a difference in the background noise level and structure depending on the survey direction. As will be discussed in later sections, this lesson was applied to the main survey. A quick preliminary survey was conducted around the boundary of each survey areas to determine the optimal survey direction prior to data collection.

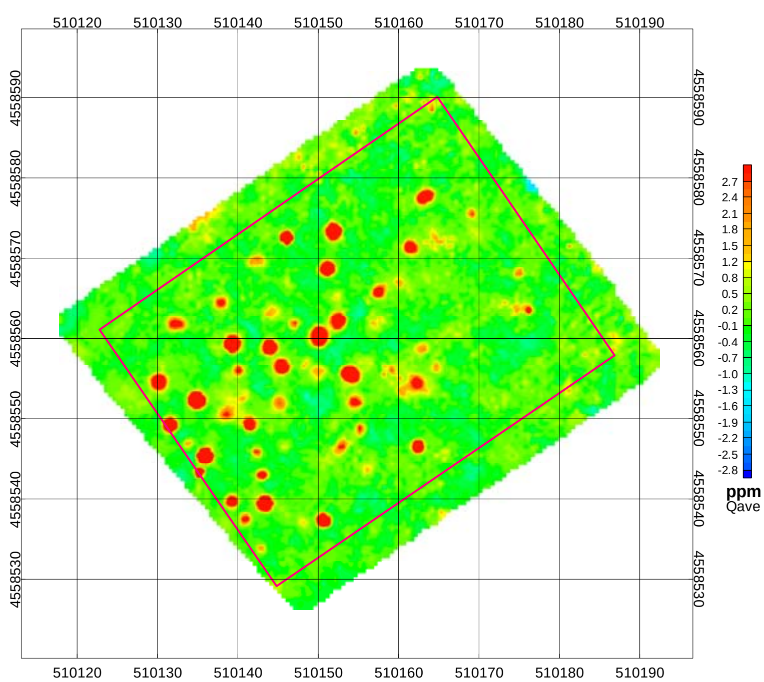


Figure 3-2 – Northwest – Southeast survey anomaly map for FEW GPO

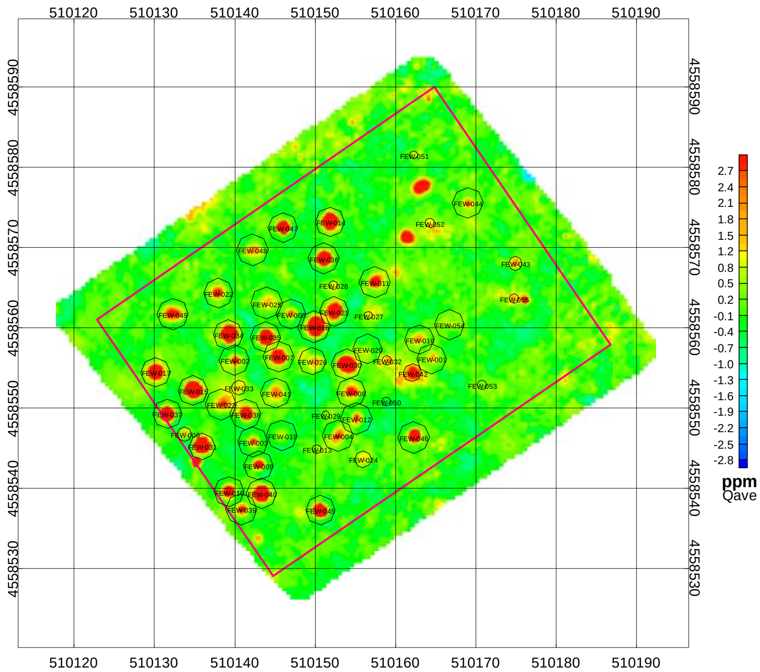


Figure 3-3 – Northwest – Southeast survey anomaly map for FEW GPO with emplaced items indicated. Note that there are also several, large-amplitude anomalies indicated that do not correspond to emplaced items.

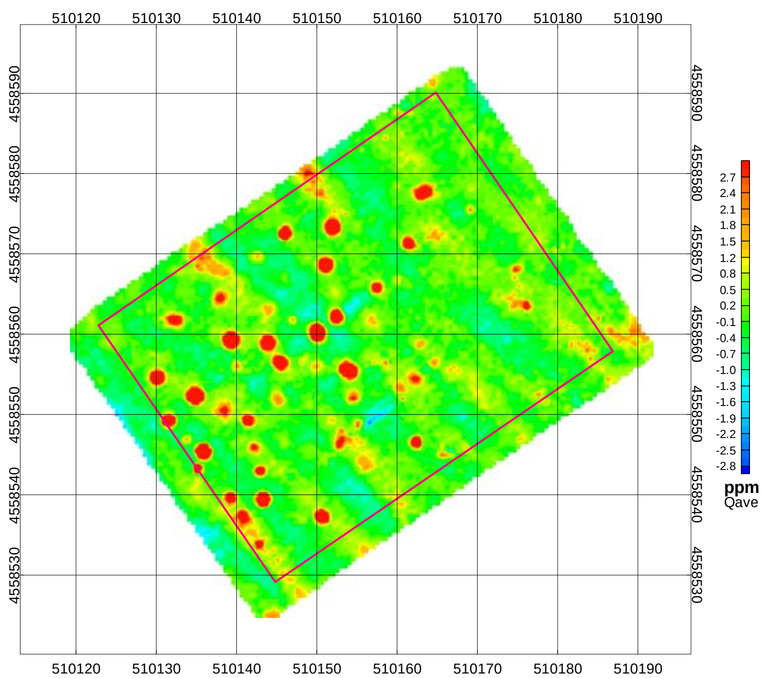


Figure 3-4 – Northeast – Southwest survey anomaly map for FEW GPO

### 3.2.6 Anomaly Detection and Detection Threshold Selection

The site-specific anomaly detection threshold for the GEMTADS array at FEW was determined in the manner similar to the one described in Section 2.1.3.2. Unlike our demonstration at the Former Camp Sibert [7], examples of each item of interest were not available for detailed measurements in a controlled manner as a function of depth. However, a GPO was available which included examples of the two items of interest for this demonstration emplaced at a variety of depths and orientations. The relevant portion of the provided ground truth for the GPO is given in Table 3-6 along with the adjusted locations, as discussed in Section 3.2.5.

Two sets of data were collected using the GEMTADS over the GPO in orthogonal directions. The use of both data sets doubles the number of observations for each item of interest to use in determining the system response. The located demedianed GEMTADS data (position, orientation, and 9 data pairs (In-phase and Quadrature response for 9 transmit frequencies)) surrounding the center of each of the relevant emplaced items were extracted and submitted to the GEMTADS solver engine. The peak value of $Q_{ave}$ for each emplaced item was also extracted. The peak $Q_{ave}$ values for the emplaced 37-mm projectile (14 observations) and the 75-mm projectile (26 observations) are shown in Figure 3-5 and Figure 3-6, respectively, as ‘x’s.

These values only represent the system responses for the observations made. To estimate the true bounds of the possible system response to the items of interest, the individual anomaly analyses are used. The resultant best-fit betas (three, $\beta$) for each item of interest are used to generate an ensemble average set of βs for each item of interest. These βs were then used to forward model the system response for the item of interest in terms of the $Q_{ave}$ quantity. Response curves were generated bounding the sensor response at the most favorable orientation and at the least favorable orientation of the sensor / item of interest pair with respect to the exciting field and as a function of depth. The response curves for the 37-mm and 75-mm projectiles are shown in Figure 3-5 and Figure 3-6, respectively. The upper curve (red) represents the sensor response (in ppm, $Q_{ave}$) for the most favorable orientation of the projectile with respect to the exciting field (the GEM-3 transmitter) as a function of depth below the surface. The sensors travel an additional 33.5 cm above the surface. The lower curve (blue) represents the response for the least favorable orientation. The measured background signal level from the GPO is also shown as a horizontal dashed line. The background signal level is given in Table 3-7. The USACE 11x level is represented as a vertical dashed line in each Figure as well.

Based on the modeled system response for each item of interest, the predicted system response for the least favorable orientation at a burial depth of 11 times the item’s diameter (11x) was determined and the results are given in Table 3-8. The least favorable response of the 37-mm projectile at a burial depth of 11x was found to be the limiting value at 1.4 ppm, $Q_{ave}$. After incorporating a safety factor of 75%, the anomaly detection threshold was set at 1.1 ppm, $Q_{ave}$, or approximately 1.8x the site-specific background signal level. The appropriateness of the anomaly detection threshold and the site background signal level were monitored throughout the demonstration, but no changes were made. The individual anomaly analysis results for the emplaced items of interest and the anomaly lists for the GPO generated using the 1.1 ppm, $Q_{ave}$ anomaly detection threshold are included on the attached CD.

As a note, emplaced items FEW-013, FEW-020, FEW-029, FEW-050, FEW-052, FEW-053 are not picked at the anomaly detection threshold of 1.1 ppm, $Q_{ave}$. Inspection of Table 3-6 shows that all of these emplaced items except FEW-050 are emplaced at depths lower than a detection would be expected based on the threshold selection criteria. There is no visible signature of item FEW-050 in either data set. Several additional anomalies are visible in the anomaly maps and were detected as well.

Table 3-6 – Partial Schedule of Emplaced Items in FEW GPO

| Target ID | Nomenclature | Orientation | Orientation Details | Depth (ft) | Northing UTM (m) | Easting UTM (m) | Northing Corrected UTM (m) | Easting Corrected UTM (m) |
|---|---|---|---|---|---|---|---|---|
| FEW-001 | Projectile, 37-mm | Vertical | Nose Up | 1.00 | 4558556.96 | 510166.71 | 4558556.15 | 510164.49 |
| FEW-002 | Projectile, 37-mm | Horizontal | Nose South | 1.00 | 4558556.82 | 510142.16 | 4558556.01 | 510139.94 |
| FEW-003 | Projectile, 37-mm | Vertical | Nose Up | 1.30 | 4558546.60 | 510144.45 | 4558545.79 | 510142.23 |
| FEW-004 | Projectile, 37-mm | Horizontal | Nose North | 1.30 | 4558547.39 | 510155.06 | 4558546.58 | 510152.84 |
| FEW-005 | Projectile, 37-mm | Vertical | Nose Up | 1.50 | 4558562.53 | 510149.21 | 4558561.72 | 510146.99 |
| FEW-006 | Projectile, 37-mm | Horizontal | Nose North | 1.50 | 4558547.59 | 510135.95 | 4558546.78 | 510133.73 |
| FEW-014 | Projectile, Shrapnel, 75-mm | Vertical | Nose Down | 1.00 | 4558573.99 | 510154.09 | 4558573.18 | 510151.87 |
| FEW-015 | Projectile, Shrapnel, 75-mm | Horizontal | Nose East | 1.00 | 4558553.01 | 510136.99 | 4558552.2 | 510134.77 |
| FEW-016 | Projectile, Shrapnel, 75-mm | Horizontal | Nose East | 2.50 | 4558559.37 | 510165.20 | 4558558.56 | 510162.98 |
| FEW-017 | Projectile, Shrapnel, 75-mm | Vertical | Nose Down | 1.50 | 4558555.29 | 510132.36 | 4558554.48 | 510130.14 |
| FEW-018 | Projectile, Shrapnel, 75-mm | Horizontal | Nose South | 1.50 | 4558560.97 | 510152.09 | 4558560.16 | 510149.87 |
| FEW-019 | Projectile, Shrapnel, 75-mm | Vertical | Nose Down | 3.00 | 4558547.43 | 510148.07 | 4558546.62 | 510145.85 |
| FEW-020 | Projectile, Shrapnel, 75-mm | Horizontal | Nose Northeast | 3.00 | 4558558.20 | 510158.75 | 4558557.39 | 510156.53 |
| FEW-034 | Projectile, Shrapnel, 75-mm | Horizontal | | 1.70 | 4558559.98 | 510141.40 | 4558559.17 | 510139.18 |
| FEW-035 | Projectile, AP, 75-mm | Vertical | | 2.00 | 4558559.69 | 510146.06 | 4558558.88 | 510143.84 |
| FEW-039 | Projectile, 37-mm | Horizontal | | 0.50 | 4558538.24 | 510143.03 | 4558537.43 | 510140.81 |
| FEW-051 | Projectile, Shrapnel, 75-mm | Vertical | Nose Up | 3.50 | 4558582.35 | 510164.51 | 4558581.54 | 510162.29 |
| FEW-052 | Projectile, Shrapnel, 75-mm | Horizontal | Nose North | 3.50 | 4558573.89 | 510166.53 | 4558573.08 | 510164.31 |
| FEW-053 | Projectile, AP, 75-mm | Vertical | Nose Down | 4.00 | 4558553.70 | 510173.01 | 4558552.89 | 510170.79 |
| FEW-054 | Projectile, AP, 75-mm | Horizontal | Nose East | 4.00 | 4558561.23 | 510168.96 | 4558560.42 | 510166.74 |

Table 3-7 – FEW GPO RMS Background Level

| Array | RMS Background Level |
|---|---|
| GEMTADS | 0.6 ppm, Qave |

Table 3-8 – System Response and Anomaly Detection Thresholds for Items of Interest

| Item of Interest | Minimum Response at 11x | Anomaly Detection Threshold |
|---|---|---|
| 37-mm Projectile | 1.4 ppm, Qave | 1.1 ppm, Qave |
| 75-mm Projectile | 2.7 ppm, Qave | 2.0 ppm, Qave |

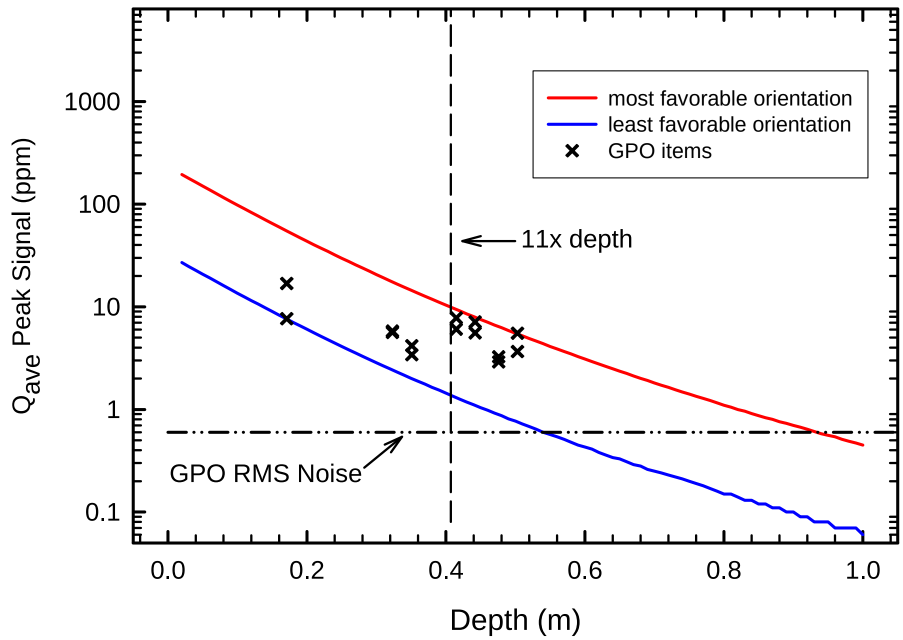


Figure 3-5 – Peak anomaly amplitude results from the MTADS GEM-3 array (GEMTADS) system and measurements of the emplaced 37-mm projectiles in the FEW GPO. The modeled system response for the most (red) and least (blue) favorable orientations of the mortar are shown as lines. The responses for the seeded GPO items are shown as 'x's. The RMS background level for the GPO and the USACE 11x rule are shown as dashed lines

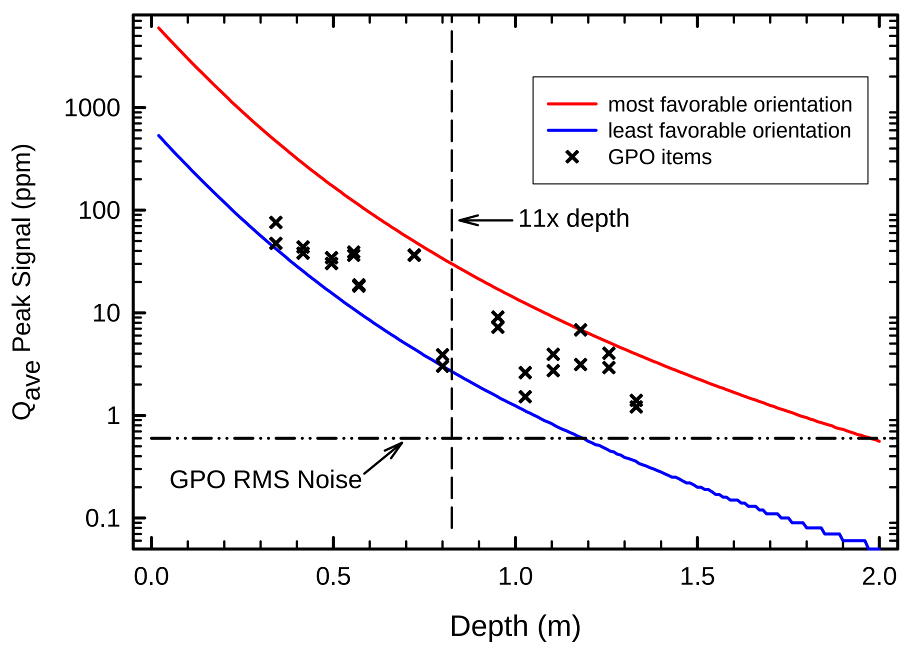


Figure 3-6 – Peak anomaly amplitude results from the MTADS GEM-3 array (GEMTADS) system and measurements of the emplaced 75-mm projectiles in the FEW GPO. The modeled system response for the most (red) and least (blue) favorable orientations of the mortar are shown as lines. The responses for the seeded GPO items are shown as 'x's. The RMS background level for the GPO and the USACE 11x rule are shown as dashed lines.

### 3.2.7 Priority Area 1 Results

The perimeter of the Priority Area 1 survey area, as shown in Figure 3-1, is a 600 ft x 600 ft area, covering 8.3 acres. The actual area surveyed is somewhat larger, covering 9.3 acres mostly due to extra data collection along the survey direction outside the original boundary. Based on the lessons learned while surveying the GPO, a quick preliminary survey was conducted around the boundary of the survey area to determine the optimal survey direction with respect to background signal level prior to data collection. The North-South survey direction was found to be the quietest survey direction. The $Q_{ave}$ anomaly map for Priority Area 1 is shown in Figure 3-7. The planning boundary is shown in pink. The As-Surveyed boundary is shown in brown. A 4.2 acre subsection of Priority Area 1 was selected for other demonstrators to survey and for the discrimination portion of this demonstration. The subset boundary is shown in orange. All anomalies within Priority Area 1 with peak $Q_{ave}$ values above the 1.1 ppm threshold are shown in Figure 3-8 as an 'x' symbol. 3,208 anomalies exceeded the threshold, and 1,395 of those anomalies were within the subset boundary and were further analyzed. All three boundaries are shown as well using the same color scheme as for Figure 3-7. The located, demedianed data archive is located on the attached CD. The anomaly list for the entire area is also located on the attached CD along with the area boundary files in Geosoft polygon file format (.ply).

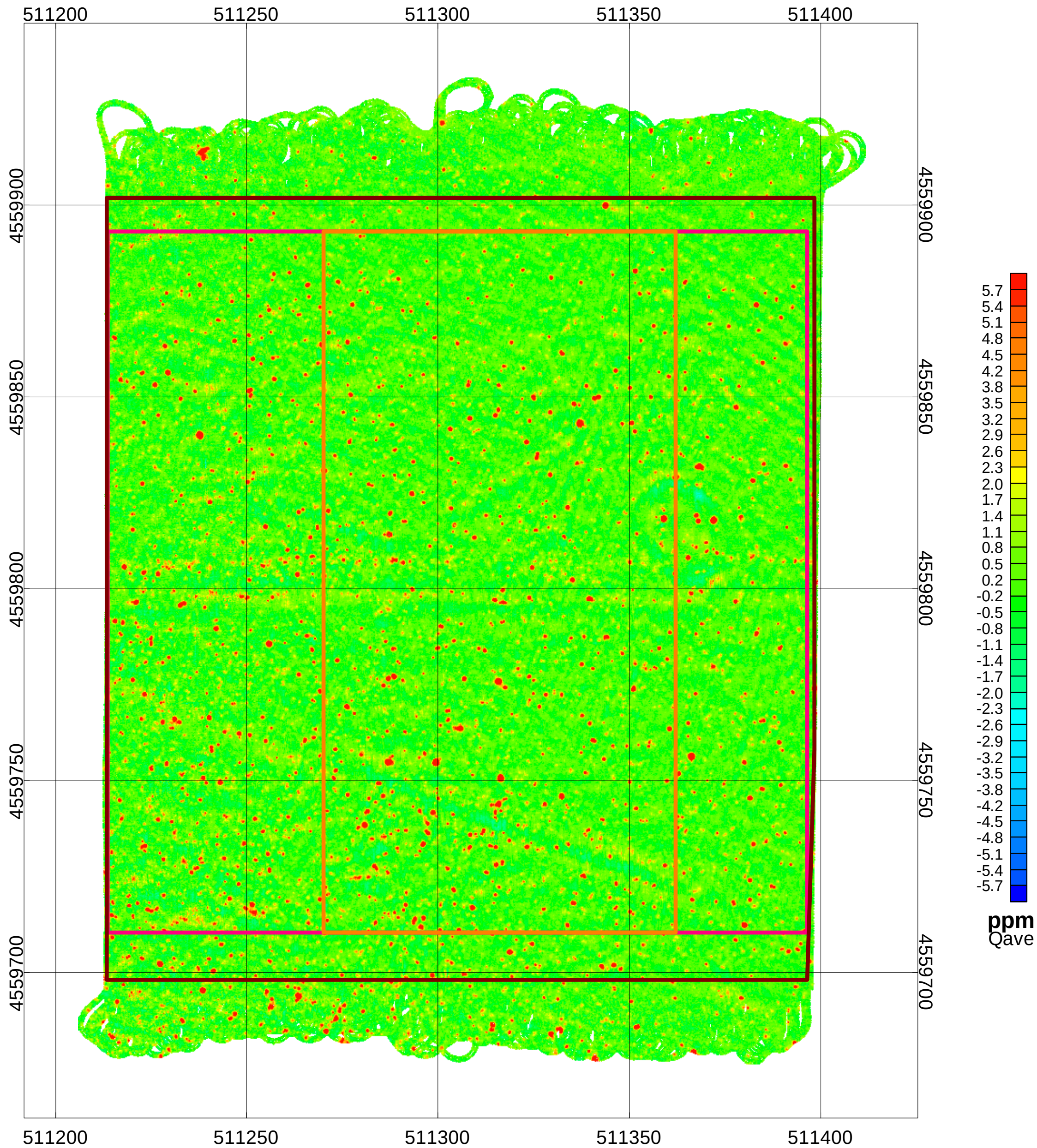


Figure 3-7 – GEMTADS anomaly map (ppm, $Q_{ave}$) for Priority Area 1. The original, planning boundary is shown in pink. The As-Surveyed boundary is shown in brown. The subset area selected for detailed data analysis and for data collection by other demonstrators is shown in orange.

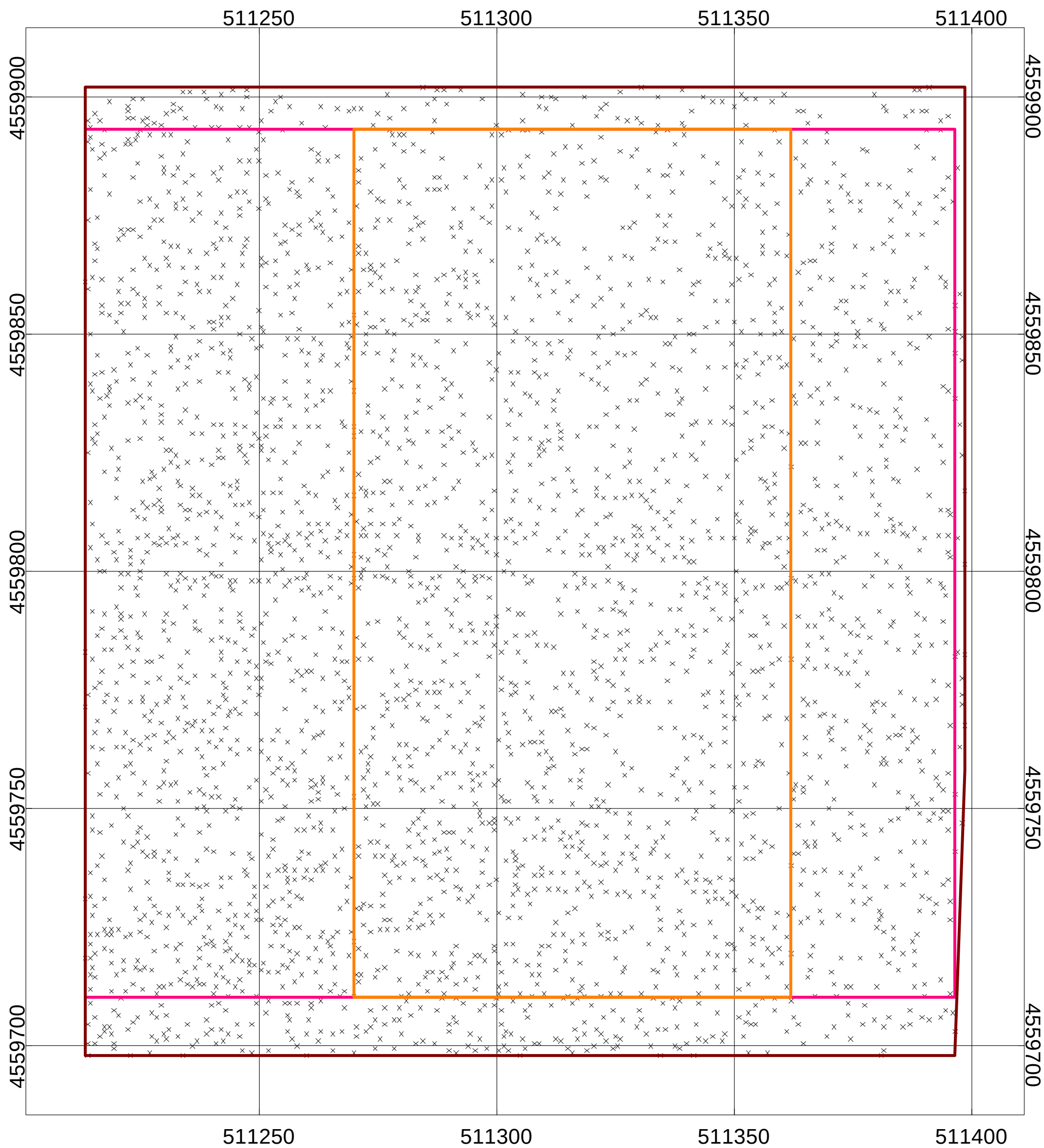


Figure 3-8 – Anomalies ('x's) above the detection threshold (1.1 ppm, $Q_{ave}$) for Priority Area 1. The original, planning boundary is shown in pink. The As-Surveyed boundary is shown in brown. The subset area selected for detailed data analysis and for data collection by other demonstrators is shown in orange.

### 3.2.8 Priority Area 2 Results

The perimeter of the Priority Area 2 survey area, as shown in Figure 3-1, is a 600 ft x 600 ft area, covering 8.3 acres. The actual area surveyed is somewhat larger, covering 9.5 acres mostly due to extra data collection along the survey direction outside the original boundary. A quick preliminary survey was conducted around the boundary of the survey area to determine the optimal survey direction with respect to background signal level prior to data collection. The North-South survey direction was found to be the best. The $Q_{ave}$ anomaly map for Priority Area 2 is shown in Figure 3-9. The planning boundary is shown in pink. The As-Surveyed boundary is shown in brown. All anomalies within Priority Area 2 with peak $Q_{ave}$ values above the 1.1 ppm threshold are shown in Figure 3-10 as an ‘x’ symbol. 5,223 anomalies exceeded the threshold. Both boundaries are shown as well using the same color scheme as for Figure 3-9. The located, demedianed data archive is located on the attached CD. The anomaly list for the entire area is also located on the attached CD along with the area boundary files in Geosoft polygon file format (.ply).

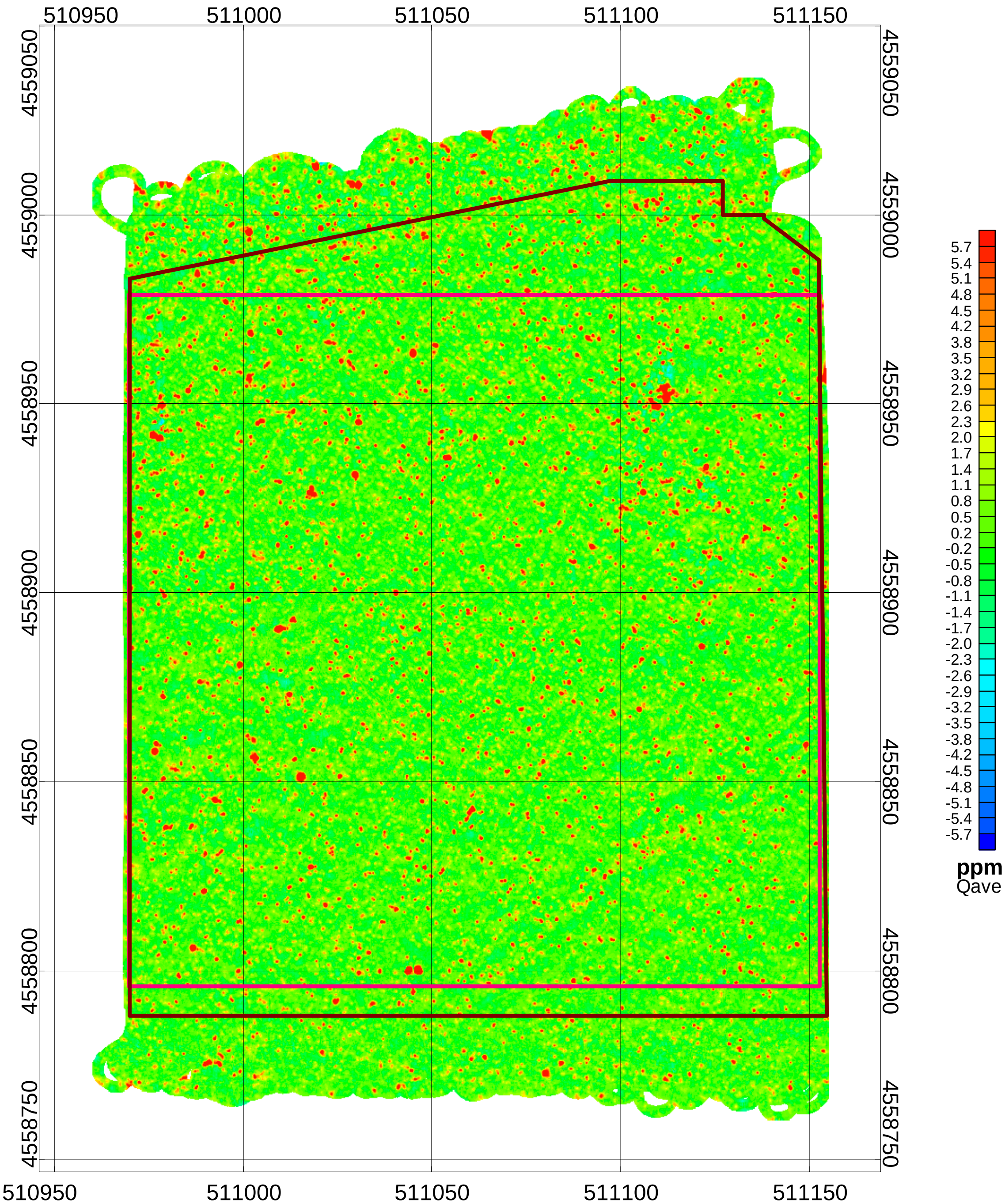


Figure 3-9 – GEMTADS anomaly map (ppm, $Q_{ave}$) for Priority Area 2. The original, planning boundary is shown in pink. The As-Surveyed boundary is shown in brown.

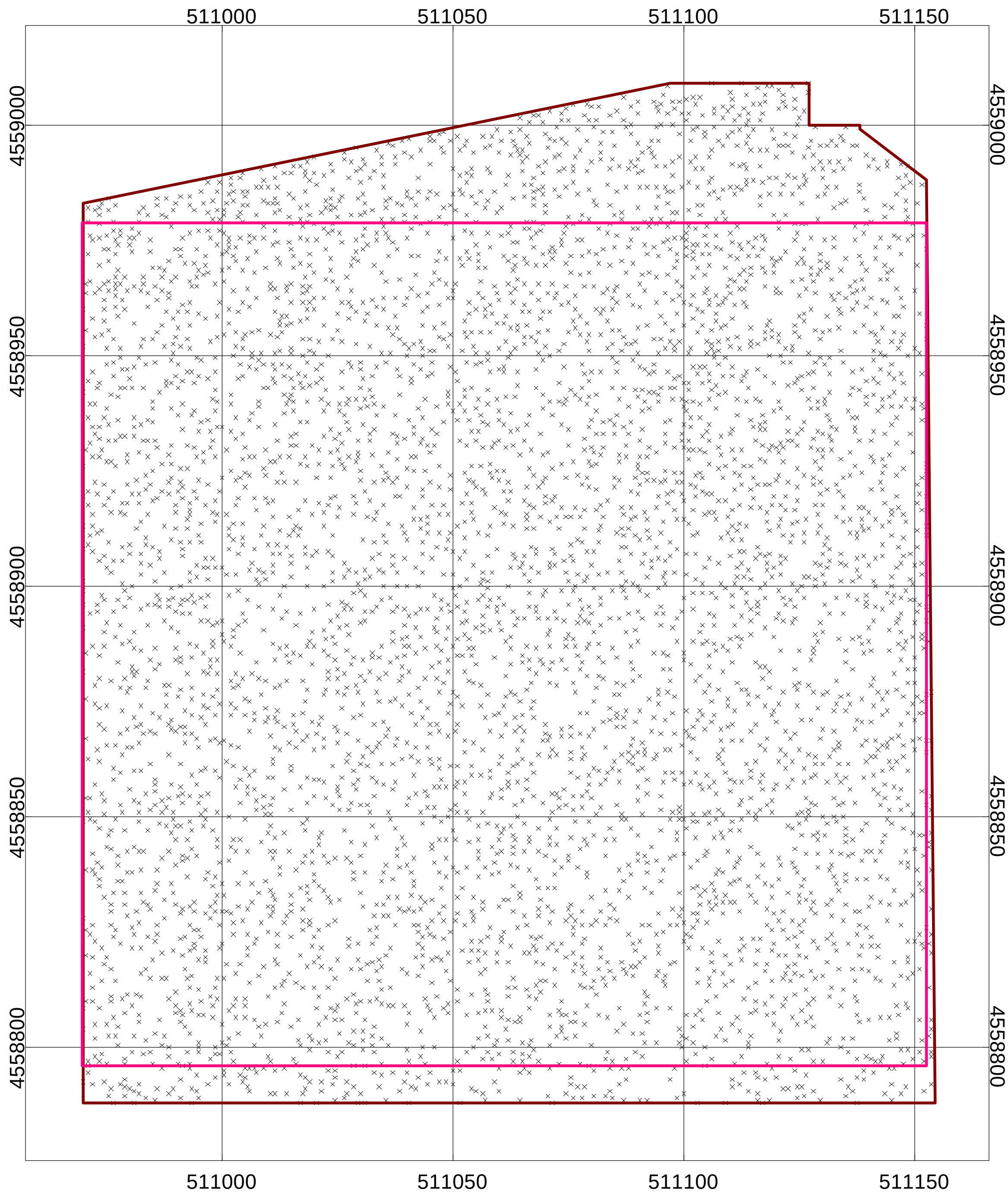


Figure 3-10 – Anomalies (‘x’s) above the detection threshold (1.1 ppm, $Q_{ave}$) for Priority Area 2. The original, planning boundary is shown in pink. The As-Surveyed boundary is shown in brown.

### 3.2.9 Priority Area 1 Subset Data Processing Results

Figure 3-11 presents the EMI data acquired over the GPO. Here, the quantity $Q_{sum}$, the sum of the middle five quadrature channels; namely, 270, 570, 1230, 2610, and 5430 Hz, is plotted. $Q_{sum}$ differs from $Q_{ave}$ by a factor of 5, $Q_{sum} = Q_{ave} / 5$, and was used by the Data Analysts for convenience. As detailed earlier, 49 UXO have been emplaced in the GPO (31 of the emplaced targets were buried less than 11x their diameter, 18 were buried deeper to characterize detection capabilities). The circles overlain on Figure 3-11 identify the locations of the emplaced targets of interest (TOI). A TOI signature library has been created using 28 high SNR anomalies from the individual anomaly analysis results.

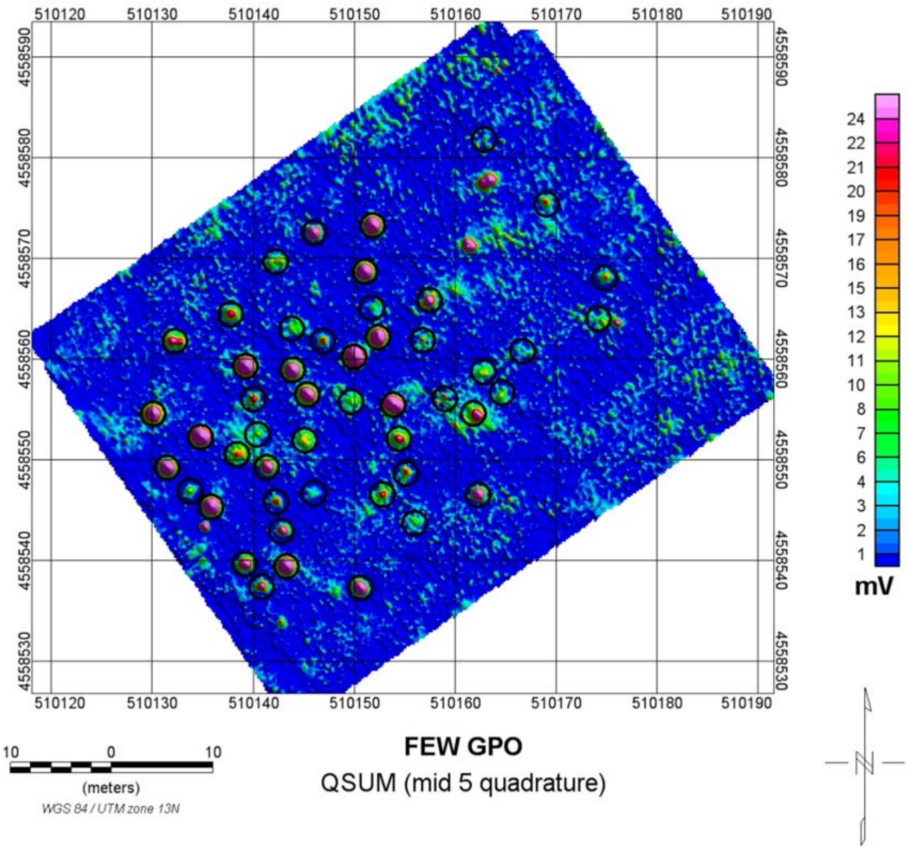


Figure 3-11 – EMI data acquired over the GPO overlain by black circles identifying seeded ordnance items

The automatic target picker described earlier identified 90 anomalies that exceeded the detection threshold in the GPO survey area, which includes all emplaced items. These additional anomaly picks are shown in Figure 3-12. Many of these anomalies do not possess a structured signal that we nominally associated with buried UXO, and are therefore most likely bad picks that will result in false alarms. Recall that the anomaly selection process was based on peak $Q_{ave}$ amplitude, and did not evaluate or use expected signal structure. To reduce the number of anomalies associated with transient signals, the dataset for each anomaly was sorted according to distance from the peak response. If seven of the first N data points (sorted first by distance from peak response and then by the next highest value) possessed $Q_{ave}$ values greater than the median value (for all data points associated with the individual anomaly) AND 3 of the first N data points possessed values of $Q_{ave}$ > median+rms (anomaly dataset median $Q_{ave}$ value plus the anomaly dataset $Q_{ave}$ rms), the anomaly was deemed to have structure and therefore to be a valid anomaly pick. This test was performed for N values of both 10 and 12. The yellow circles in

Figure 3-12 identify non-seeded target picks that were rejected from the list of candidate targets based on these rules.

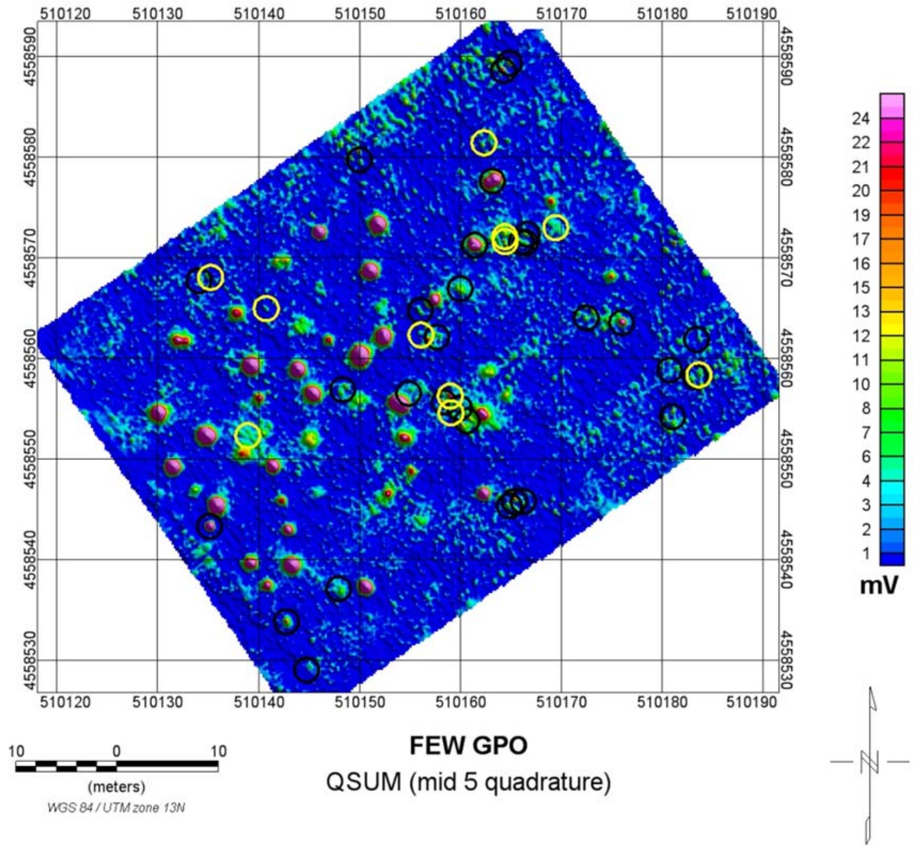


Figure 3-12 – EMI data acquired over the GPO overlain by anomaly picks that are not associated with a seeded item. Yellow circles identify picked targets that were subsequently rejected based on statistical rules evaluating peak signal strength and local spatial variance.

Figure 3-13 presents fitted results for the emplaced UXO in the GPO. Here, we plot the fitted mismatch, defined as SQRT(1-correlation coefficient^2), versus the coherence ratio. The coherence ratio is defined as the best-fit library coherence divided by the unconstrained fit coherence. It ranges from 0 to 1 where 0 indicates that the anomaly under investigation cannot be modeled well using the fixed polarizations included in the TOI library. The red symbols in Figure 3-13 identify anomalies that have fit errors of less than 50% and fitted depths of less than 0.75m. The blue symbols identify anomalies that exceed these thresholds. Anomalies that exceed these thresholds will be ranked Category 3 and recommended to be dug. The solid blue line limits to the mean value of the coherence ratio for high SNR seeded items. The dashed line is shifted down from the mean by four standard deviations. Color coded symbols in Figure 3-14 identify anomalies in the two-dimensional mapped data above and below this threshold.

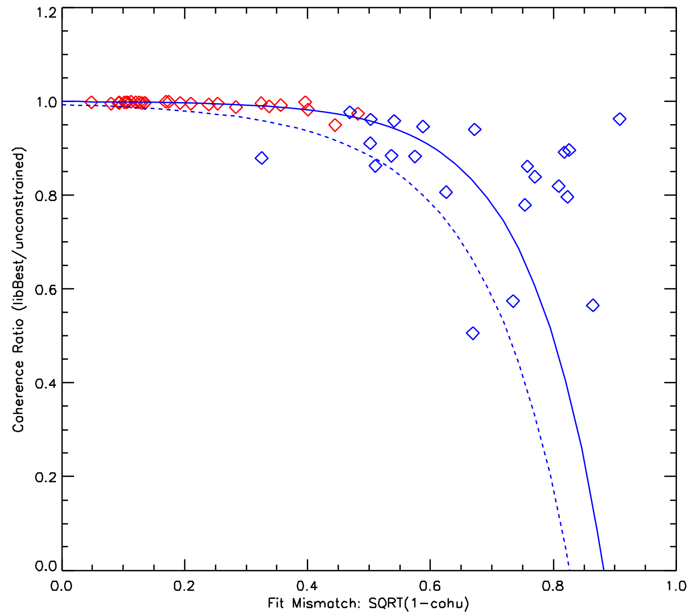


Figure 3-13 – Scatter plot of the fit mismatch versus coherence ratio for emplaced UXO in the GPO area. The red symbols identify anomalies with a fit error of less than 50% and fitted depths of less than 0.75 m. The blue symbols identify anomalies that exceed these thresholds. See text for discussion.

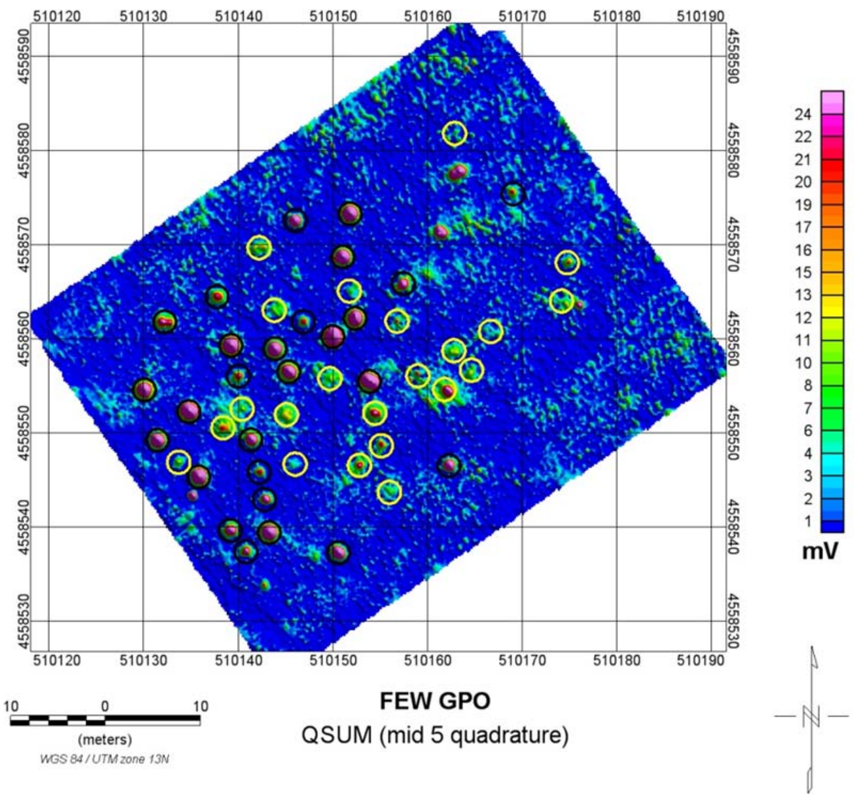


Figure 3-14 – EMI data acquired over the GPO overlain by circles identifying seeded ordnance items. The black circles identify targets with fit errors less than 50% and fitted depths less than 0.75 m. The yellow circles identify seeded UXO that exceed these thresholds.

Figure 3-15 shows the fit error versus signal strength for all targets in the GPO and PA1 subset survey areas. Here, signal strength is defined as $Q_{ave}$, the average quadrature response for the middle five frequencies. As expected, we observe larger fit errors with decreasing signal strength. Figure 3-16 superimposes data from the PA1 subset area on Figure 3-13.

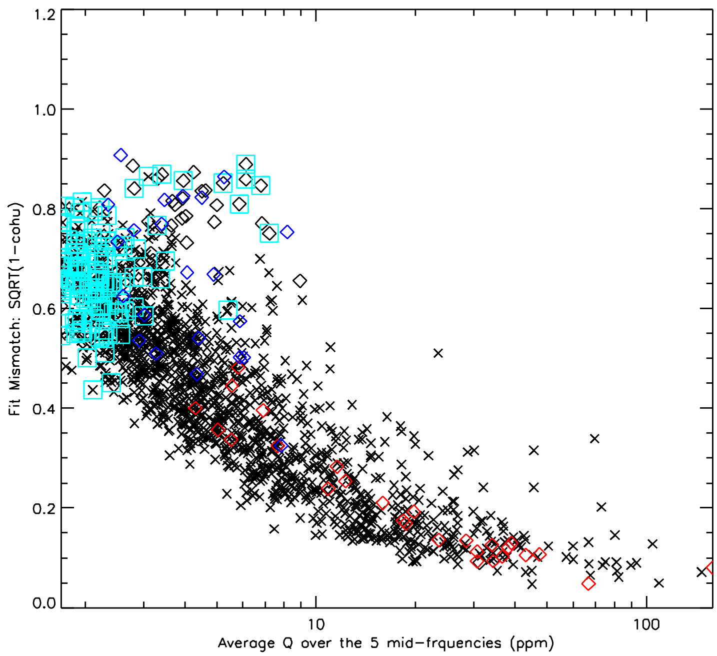


Figure 3-15 – Fitted results from the GPO (diamond symbols) and PA1 subset (x symbols) survey areas. Red color is used to identify high SNR targets in the GPO, blue is low SNR, black unknown, and cyan identifies targets that passed the detection threshold but were later rejected based on statistical rules.

Fitted results in the feature space proposed for decision making are shown in Figure 3-17. Here, we plot the fit mismatch versus the relative coherence ratio normalized by the standard deviation about the mean for the library TOIs. Anomalies with fit errors larger than 50% will be ranked Category 3 unless rejected by our statistical rules as an invalid detection pick. For anomalies with fit errors less than 50%, we propose basing the discrimination decision on the coherence ratio as shown. Because the library consisted of TOI only, items similar to those in the library will possess ratios close to one. Objects that cannot be represented by the TOI polarizabilities have ratios less than one. Based in part on trial and error, we selected a Category 1-2 threshold of -4. Based on these limited training data, this threshold captures all labeled UXO not excluded due to low SNR. Figure 3-18 focuses on the labeled UXO items only in Figure 3-17 and shows that all labeled UXO are located above a threshold of -2, leaving a margin of safety when using a threshold of -4.

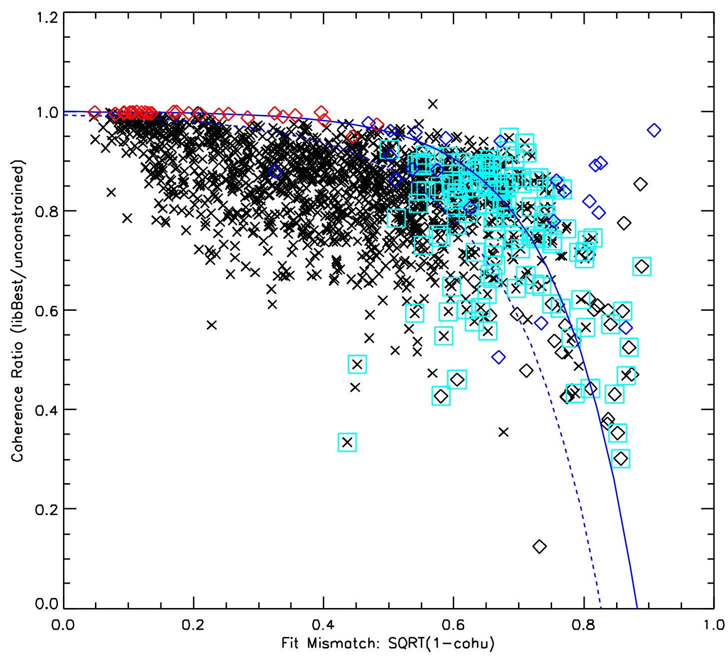


Figure 3-16 – Fitted results from PA1 subset area are superimposed on the fitted results from the GPO.

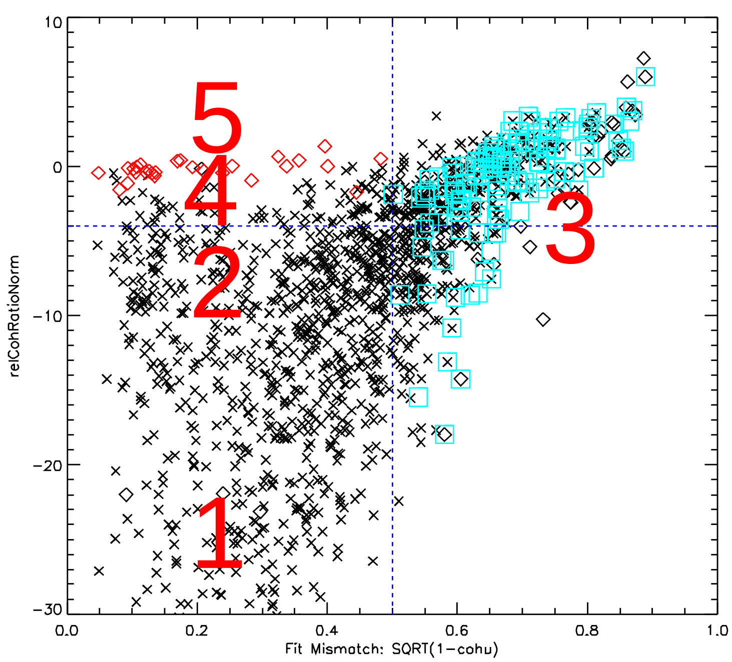


Figure 3-17 – Scatter plot of fit results for anomalies in PA1 subset and GPO areas. See text for description.

These results appear promising, but cannot be used to predict the expected performance for two reasons. First, the training data do not include any non UXO objects. Because of this we cannot say anything about the separation between TOI and non-TOIs. Second, we are not confident that the distribution of labeled data in the GPO adequately reflects the distribution of unknown targets in the PA1 subset area. If labeled training data were available from the PA1 subset area, the discrimination decision criteria discussed above could be further refined. Depending on the actual distribution of UXO in the PA1 subset area, it might be possible to revise the GPO-based detection threshold upwards and thereby reduce the number of items placed in Category 3. Additionally, the detection threshold decision could also be revisited.

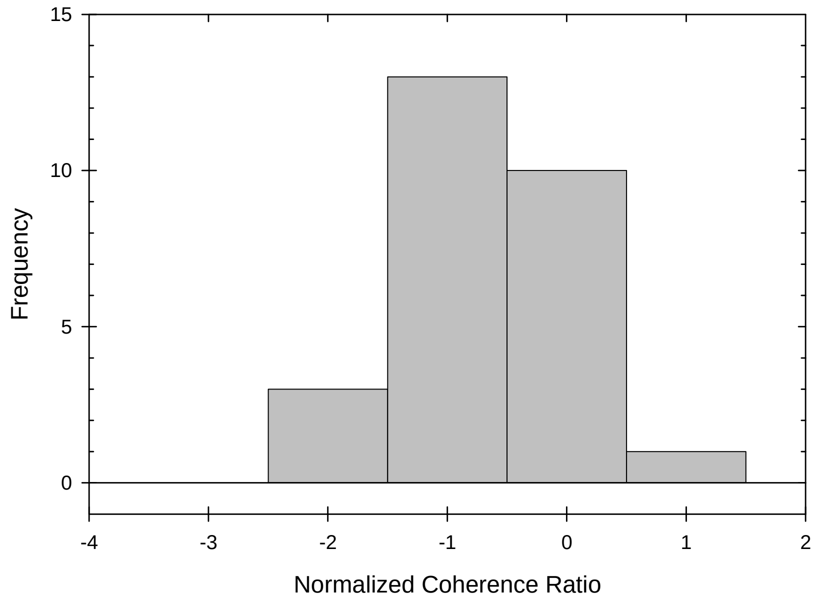


Figure 3-18 – Histogram showing the frequency of labeled UXO as a function of the decision metric. As shown, all labeled UXO not excluded based in SNR posses values greater than -2.

### 3.2.10 Systems Performance and Calibration Item Results

For the GEMTADS array, the standard performance checks included three types of measurements. At the beginning of field work and again each morning; quiet, static data were collected for a period (5 minutes or as directed by the QAO) with all systems powered up and warmed up (20 minutes minimum). Next, two calibration items, a 4” diameter Aluminum (Al) sphere and a ferrite rod bundle, were placed a standard distance above the center of each sensor coil several times in sequence to verify the response of each sensor to each object. The system was kept stationary for this data collection. Finally, a systems timing check using a fixed-position chain placed on the ground was conducted. The timing check and the Al sphere and ferrite measurements were repeated at the end of each survey day.

Two pieces of data are extracted from the stationary data, the position variation and the GEM-3 sensor variation. It should be noted that the sensor platform was only deployed for a few days, so the variations reported do not have a large enough sample size to be statistically relevant. However, the reported values are instructive, taken in that context. The 2-D position variation was evaluated by computing the standard deviation of both the northing and easting components of the position data for the entire period and combining them as the square root of the sum of the squares. The 3-D position variation was calculated in a similar manner by adding the vertical (HAE) measurement. The standard deviation for the demedianed sensor data from each sensor was computed and the arithmetic mean was computed for each data set. The aggregate average and standard deviation (1σ) of both the positioning and sensor data for all data sets were computed. The results are shown in the following time-series figures. Figure 3-19 shows the 2-D position variation for the entire demonstration, which is summarized in tabulated in Table 3-9 along with the 3-D variation.

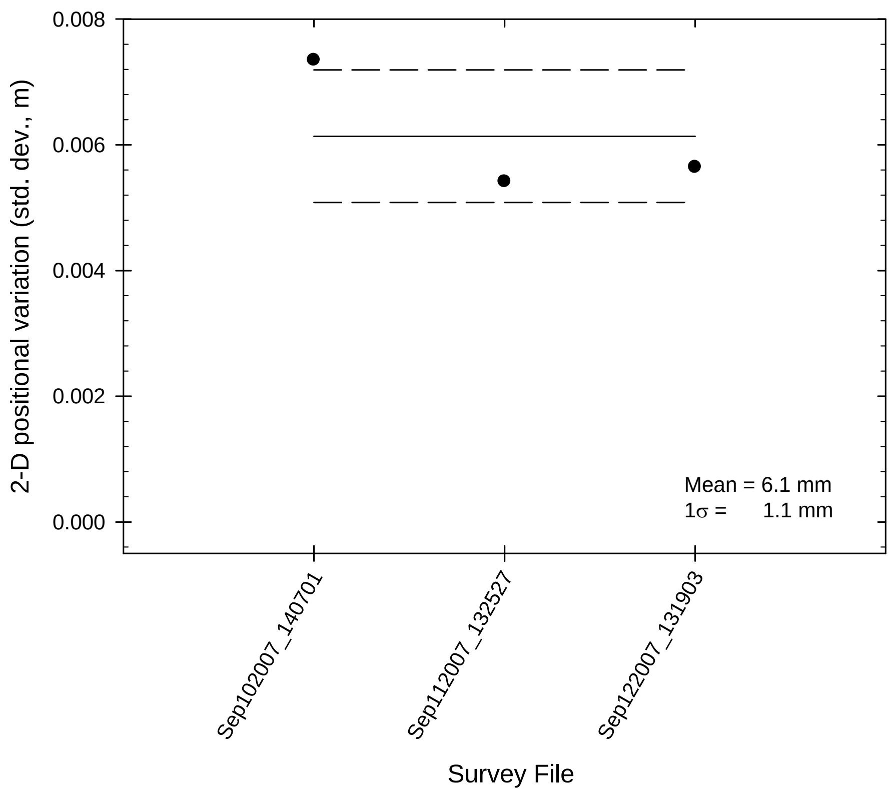


Figure 3-19 – 2-D position variation data runs for stationary data collected near the base camp. The horizontal axis is survey file name. The solid line represents the aggregate average positional variation and the dashed lines represent a 1σ envelope.

Table 3-9 – FEW Base Camp Stationary Position Variation Results

| Result Type | Value |
|---|---|
| 2-D Position | 0.61 ± 0.11 cm |
| 3-D Position | 0.93 ± 0.09 cm |

Figure 3-20 show the sensor variation from the stationary data collections for the GEMTADS array. Table 3-10 summarizes the stationary GEM-3 sensor data collection results. The quantity $Q_{ave}$ is calculated for each sensor and then the results are averaged for the run.

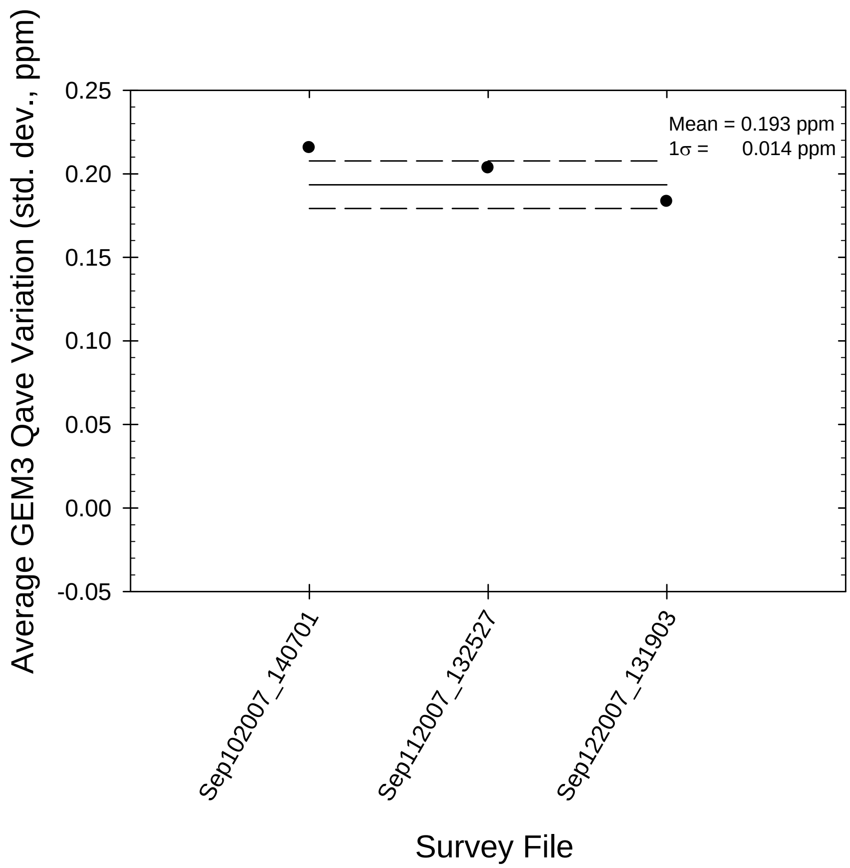


Figure 3-20 – GEM-3 sensor variation for stationary data collected near the base camp. The horizontal axis is survey file name. The solid line represents the aggregate average positional variation and the dashed lines represent a 1σ envelope.

Table 3-10 – GEM-3 (GEMTADS) Array Static Test Data Results (demedianed values)

| Result Type | Value |
|---|---|
| $Q_{ave}$ | 0.193 ± 0.014 ppm |

For the 4” dia. Al sphere, the sphere was placed a standard distance above the center of each sensor several times to measure the response of each sensor. Any background level is removed using a demedian filter. The quantity $Q_{ave}$ was then calculated and used for this discussion. The average of all measurements with the sphere for each sensor within a survey is calculated. The average amplitude value for each survey / sensor pair (average and standard deviation (1σ)) is tabulated in Table 3-11.

Table 3-11 – Average Demedianed GEMTADS Response for the 4-in Al Sphere

| Item | Avg. Signal (Qave, ppm) | Std. Dev (Qave, ppm, 1σ) |
|---|---|---|
| 4-in Al Sphere Coil 1 | 283.95 | 5.3 |
| 4-in Al Sphere Coil 2 | 285.18 | 5.5 |
| 4-in Al Sphere Coil 3 | 285.33 | 4.4 |

Figure 3-21 plots the average response amplitude the 4-in Aluminum Sphere for all data sets in a time series. The results for each coil are shown as colored symbols using the standard color coding. The variations are small and in many cases, the symbols overlap. The solid line indicates the aggregate average for all measurements and the dashed lines indicate a 1σ envelope.

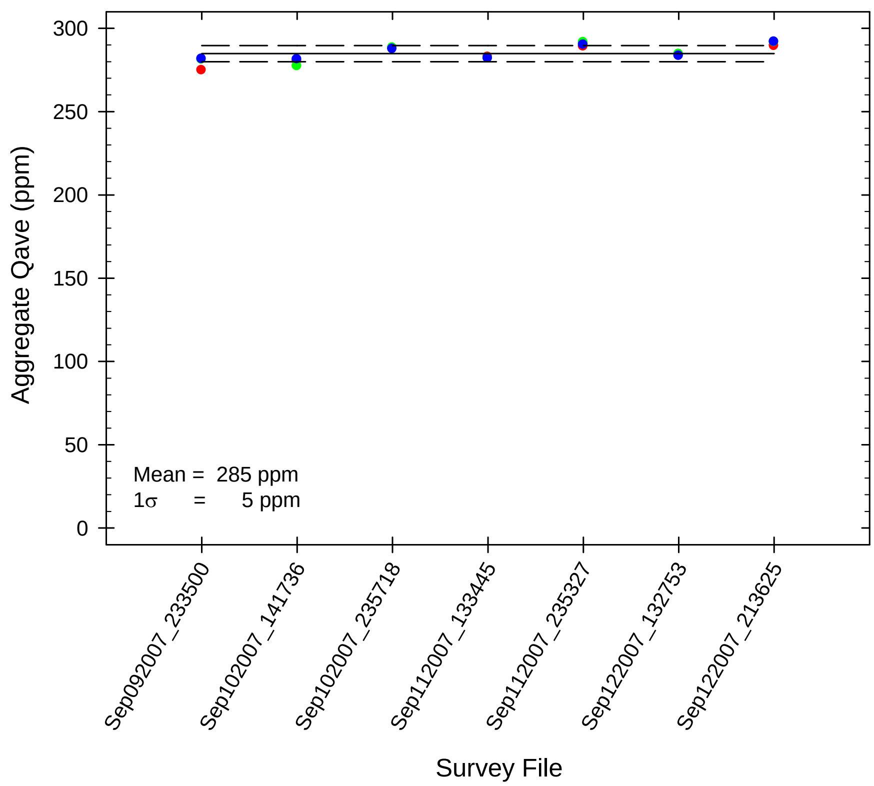


Figure 3-21 – Overall variation of GEMTADS, $Q_{ave}$ value for daily stationary data collection. The horizontal axis is survey file name. The solid line represents the aggregate average sensor variation and the dashed lines represent a 1σ envelope. The symbols represent each sensor / survey data pair. The symbol color code is the standard one described previously in the text.

### 3.2.11 Demobilization

At the end of field operations, all NRL equipment, materials, and supplies were packed in the 53' trailer. A government-contracted transportation company picked up the trailer prior to the field personnel departing the site. The 53' trailer was delivered to Blossom Point, MD as indicated in Table 3-4. URS had previously arranged for the delivery of the portable toilet and arranged for the removal after field operations were completed. The shipping container was left in place for the next demonstrator and was removed when no longer required.

#### 3.2.12 Health and Safety Plan (HASP)

A host organization exists for this demonstration site. URS Corporation, Inc. has prepared a Project Health and Safety Plan [11] and an Explosives Safety Submission [9] in cooperation with FEW and AFCEE as part of their involvement in the ongoing RI. This demonstration was conducted under the authority of this Health and Safety Plan in coordination with URS and FEW.

### 3.3 Management and Staffing

The responsibilities for this demonstration are outlined in Figure 3-22. Dr. Daniel Steinhurst is the PI of this project and filled the roles of Site / Project Supervisor and Quality Assurance Officer. Mr. Glenn Harbaugh was the Site Safety Officer and Data Acquisition Operator. His duties included data collection and safety oversight for the entire team. Dr. Nagi Khadr is the Data Analyst for this effort.

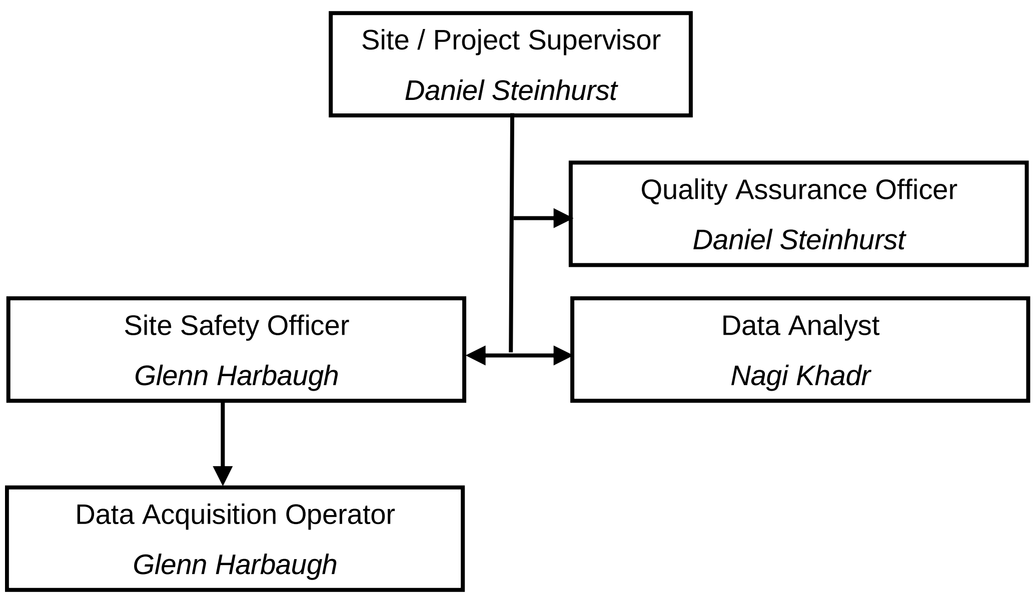


Figure 3-22 – Management and staffing wiring diagram

# 4. References


1. "Moving Platform Orientation for an Unexploded Ordnance Discrimination System," D. Steinhurst, N. Khadr, B. Barrow, and H. Nelson, *GPS World*, **2005**, *16/5*, 28 – 34.

2. "Airborne MTADS Demonstration at the Badlands Bombing Range, September, 2001," J.R. McDonald, D.J. Wright, N. Khadr, H.H. Nelson, NRL/PU/6110—02-453.

3. "SAIC Analysis of Survey Data Acquired at Camp Sibert, Interim Letter Report, Version 2," July, 2008. http://serdp-estcp.org/content/download/5529/76987/file/MM-0210

4. "Advanced MTADS Classification for Detection and Discrimination of UXO," H.H. Nelson, T.H. Bell, J.R. McDonald, B. Barrow, NRL/MR-MM/6110—03-8663. http://serdp-estcp.org/content/download/5568/77347/file/UX-4003-FR-01.pdf

5. "Enhanced UXO Discrimination Using Frequency-Domain Electromagnetic Induction," ESTCP MM-0033 Final Report, May, 2007. http://serdp-estcp.org/content/download/5576/77411/file/MM-0033-FR.pdf

6. "Survey of Munitions Response Technologies," ESTCP, ITRC, and SERDP, June, 2006. http://serdp-estcp.org/content/download/8565/104843/file/Survey_of_MR_Tech.pdf

7. "MTADS Demonstration at Camp Sibert Magnetometer / EM61 MkII / GEM-3 Arrays," Demonstration Data Report, G.R. Harbaugh, D.A. Steinhurst, N. Khadr, August, 2008. http://serdp-estcp.org/content/download/5614/77761/file/MM-0533-GEM-Data.pdf

8. "ESTCP Pilot Program, Classification Approaches in Munitions Response," H.H Nelson, K. Kaye, A. Andrews, November 17, 2008. http://serdp-estcp.org/content/download/7423/94821/version/1/file/ESTCP-Classification-CampSibert-FinalReport+12-17-09.pdf

9. "Explosive Safety Submission for the Closed Base Ranges, F.E. Warren Air Force Base, Wyoming," prepared by URS Group, Inc., August 2004.

10. *Range Reconnaissance Work Plan*, F.E. Warren Air Force Base, WY, USAF, September 2003.

11. "Project Health and Safety Plan for Remedial Investigation at the Firing Range at F.E. Warren Air Force Base, Cheyenne, Wyoming," prepared by URS Group, Inc., January 2004.

# 5. Points of Contact

**ESTCP**

| | | |
|---|---|---|
| Anne Andrews | Program Manager, MM | Tel: 703-696-3826<br>Fax: 703-696-2114<br>anne.andrews@osd.mil |
| Katherine Kaye | Program Assistant, MM | Tel: 410-884-4447<br>Fax: 703-478-0526<br>kkaye@hgl.com |

**F.E. Warren AFB**

| | | |
|---|---|---|
| John Wright | Chief of Environmental Restoration,<br>F.E. Warren Air Force Base | Tel: 307-773-4147<br>john.wright@warren.af.mil |
| Brian Powers | Group Leader, Environmental Investigation<br>URS Corporation | Tel: 303-694-2770<br>Fax: 303-694-3946<br>Cell: 303-618-7395<br>brian_powers@urscorp.com |

**NRL**

| | | |
|---|---|---|
| H. H. Nelson | Project Manager, WAA | Tel: 202-767-3686<br>Fax: 202-404-8119<br>Cell: 202-215-4844<br>herb.nelson@nrl.navy.mil |

**Nova Research, Inc.**

| | | |
|---|---|---|
| Dan Steinhurst | Principle Investigator | Tel: 202-767-3556<br>Fax: 202-404-8119<br>Cell: 703-850-5217<br>dan.steinhurst@nrl.navy.mil |
| Glenn Harbaugh | Site Safety Officer | Tel: 301-392-1702<br>Fax: 301-392-1702<br>Cell: 804-761-5904<br>roo749@yahoo.com |
| Russell Jeffries | Logistics Support | Tel: 703-360-3900<br>Fax: 703-360-3911<br>Cell: 703-244-1245<br>rjeffries@novaresearchonline.com |

**SAIC, Inc.**

| | | |
|---|---|---|
| Nagi Khadr | Data Analyst | Tel: 703-413-0500<br>Fax: 703-413-0505<br>nagi.khadr@saic.com |

**Hotel Accommodations**

| | | |
|---|---|---|
| La Quinta Inn Cheyenne | | 2410 W. Lincolnway<br>Cheyenne, WY 82009-3301<br>Tel: 307-632-7117<br>Fax: 307-638-7807 |

# Appendix A. GEMTADS Performance at the Standardized UXO Technology Demonstration Sites

The NRL GEMTADS array was developed under ESTCP Project MM-0033. The project objective was to demonstrate the optimum system built around the Geophex GEM-3 EMI sensor that delivers the most classification performance while retaining acceptable survey efficiency. A three-sensor array system was designed around a modified GEM-3 sensor. The system was built and characterized and then demonstrated at the Standardized UXO Demonstration sites at Aberdeen Proving Ground and Yuma Proving Ground. At each of the sites, the Calibration Lanes, the Blind Test Grid, and as much of the Open Field Area as was possible were surveyed. For the Blind Test Grid and the Open Field, the ranked target picks were submitted to Aberdeen Test Center for scoring. These scoring results are the basis for characterizing the success of the demonstrations and the performance of the array. Portions of Reference 5 are reproduced here to summarize the performance of the system.

## A.1 Aberdeen Proving Ground Blind Grid

### A.1.1 Response Stage

The first stage of scoring at the Test Sites is the Response Stage where anomalies are identified, or detected. For this, we use the $Q_{avg}$ quantity; the average of the quadrature response for the middle five frequencies.

$$Q_{avg} = \frac{\sum (Q_{270Hz} + Q_{570Hz} + Q_{1230Hz} + Q_{2610Hz} + Q_{5430Hz})}{5}$$

We choose this metric because of the lower noise in the quadrature response and the good signal in the mid frequencies for the objects of interest. A $Q_{avg}$ plot for the APG Blind Grid is shown in Figure A-1. The 400 cells in the Blind Grid are marked with white squares in Figure A-1. A summary of the GEM array detection performance is given in Table A-1.

Table A-1 – Summary of Detection Performance at the APG Blind Grid.

| **Cell Contents** | **Number of Cells** | **Number Correct** | **Number Incorrect** |
|---|---|---|---|
| Single Ordnance Item | 84 | 73 | 11 |
| Ordnance Item with Clutter | 7 | 7 | 0 |
| Single Clutter Item | 95 | 91 | 4 |
| Two Clutter Items | 8 | 8 | 0 |
| “Empty” | 206 | 174 | 32 |
| **Total** | **400** | | |

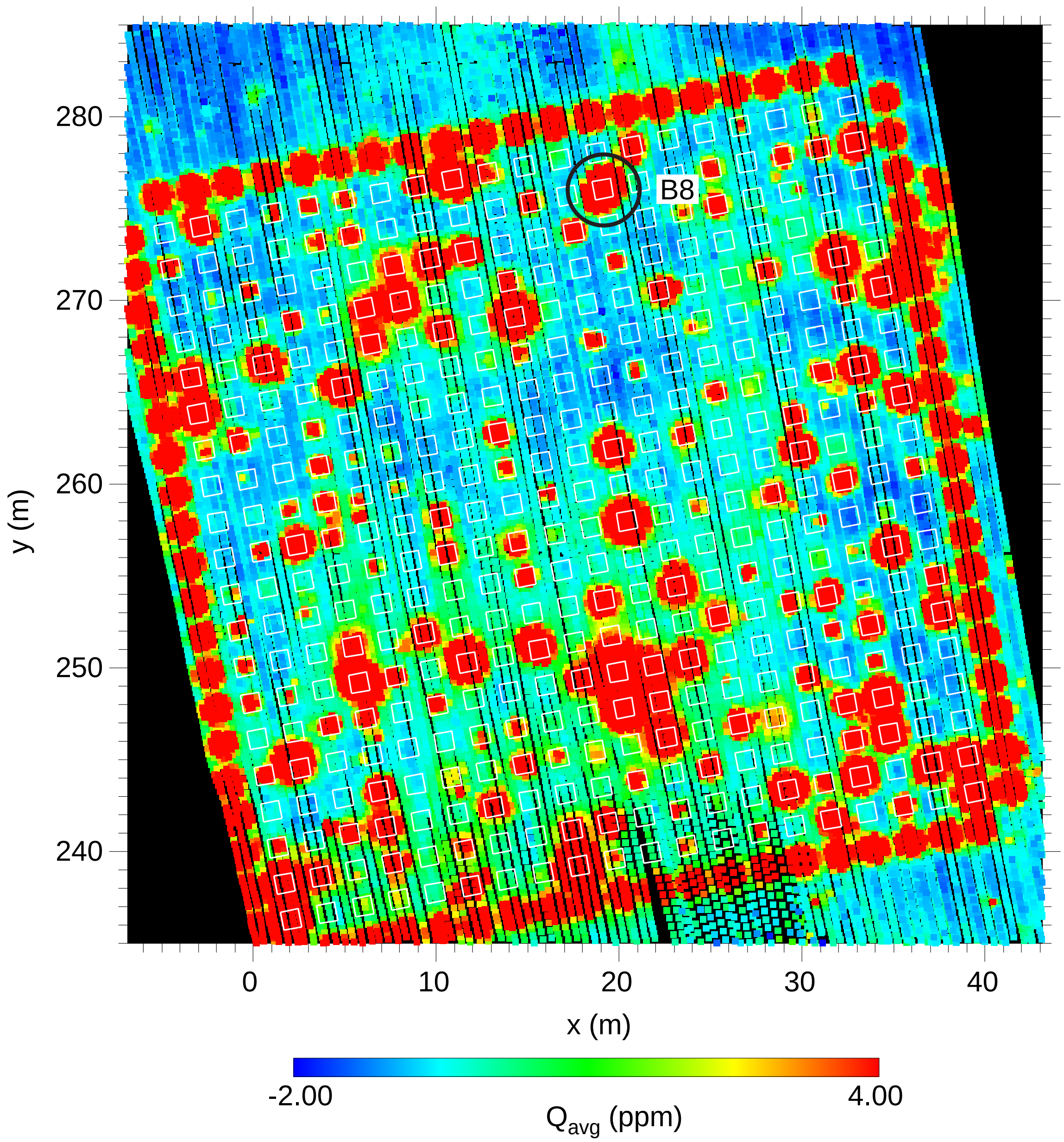


Figure A-1 – $Q_{avg}$ anomaly image map of the APG Blind Grid

The 32 cells reported as “Empty” but for which we made a declaration require some discussion. Only 12 of these false positives showed signal in the GEM array survey only. Seven of these cells had a detection by the GEM array, the EM61 HH, and the magnetometer array. Ten had a detection by the GEM array and the EM61 HH and 3 had a detection by the GEM array and the magnetometer array. An example of this is cell B8 which is highlighted in Figure A-1. It is difficult to understand the observed signal unless there is some inadvertent metal in this cell.

An indication of the depth performance of the system is shown in Figure A-2. The detected items are shown as black triangles and the missed items are shown as red crosses. The reference line corresponds to a depth of 11x the item diameter. As can be seen, the GEM array is capable of detecting targets down to and below 11 times their diameter at this site.

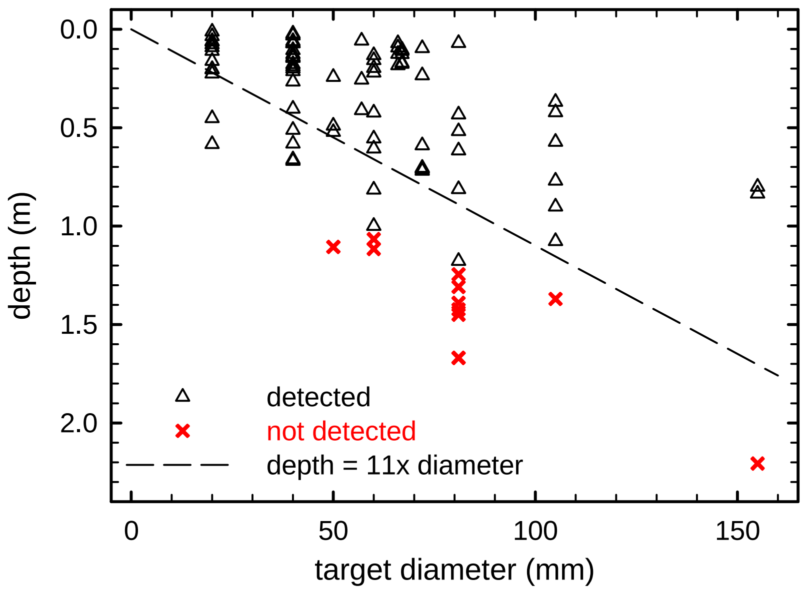


Figure A-2 – $Q_{avg}$ Detection performance as a function of depth at the APG Blind Grid

The response stage data are plotted in Figure A-3 and Figure A-4 in the manner of the Standardized Test Site scoring reports. Figure A-3 shows cumulative ordnance count vs. cumulative clutter count. Since the targets are ordered by signal amplitude at the response stage it is no surprise that this plot is essentially along the diagonal.

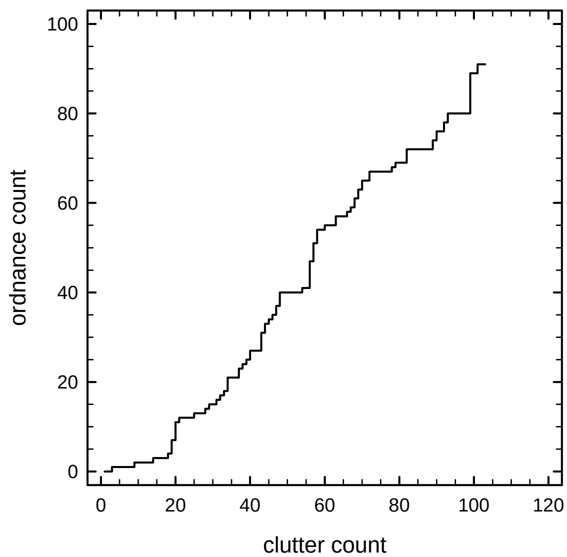


Figure A-3 – Response stage results showing cumulative ordnance count vs. cumulative clutter

A better measure of system capability is shown in Figure A-4 which plots cumulative occupied cells vs. adjusted cumulative blank cells. Cells such as B8 which obviously contain buried metal were excluded from the blank count.

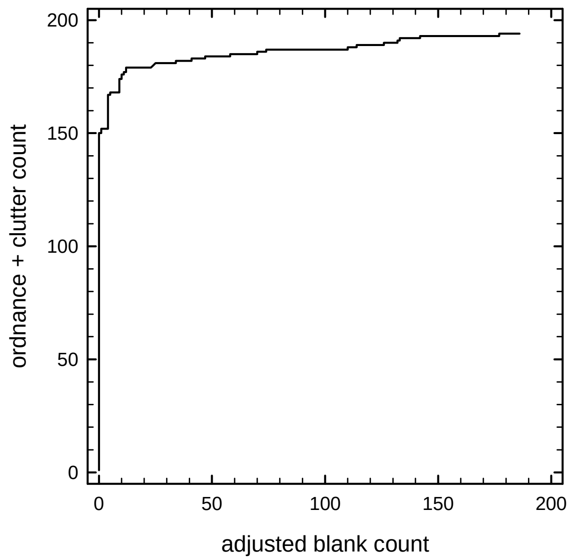


Figure A-4 – Response stage performance showing cumulative occupied cell count plotted vs. adjusted cumulative blank cell count

### A.1.2 Discrimination Stage

The prescription for discrimination using GEMTADS is to compare the measured response of a target to each of a set of library response functions in turn, and to determine which library item results in the closest match to the target. If the match is good enough, we can declare the target as being that member of the library. To quantify the "goodness-of-fit", we compute the $\chi^2$ for the each match. For the APG Blind Grid, three different methods of discrimination based on the $\chi^2$ were evaluated.

The first method is one based on the weighing of the $\chi^2$ by the signal amplitude. If the signal level for the various targets differs by a large amount (some targets quite shallow and some very deep) the computed $\chi^2$ can be strongly affected by the signal amplitude. To test this possibility, we computed the $\chi^2$ for the best match weighting the data by the usual $1/\text{rms}^2$ (where the rms deviation is determined from areas between targets) and by 1/(rms + 0.01 x signal) in an attempt to reduce the influence of depth on the computed $\chi^2$. The $\chi^2$ calculated with the signal-based weighting was used for our declarations at the APG Blind Grid. Based on the results from the Calibration Lanes (which was all we had available at the time), we established a $\chi^2$ threshold of 0.01 for the ordnance/clutter decisions. This is a little less than three standard deviations above the ordnance mean. The reported Discrimination Response Factor was just the inverse of the $\chi^2$.

The second method assumes that this strong variation of $\chi^2$ with signal amplitude arises from the bouncing motion of the sensor array as it traverses the rough field. Over a high-signal target, small variations in *z* result in relatively large variations in signal as compared to over a deep, low-signal target. In this case, we can model the bouncing noise by (K * signal) and the correct weighting would be $1/(\text{rms}^2 + (K * \text{signal})^2)$. Based on data collected on the Blossom Point Test Field, at values of K around 0.3, the scaling of $\chi^2$ with signal amplitude seems to flatten out.

Scaling the weights by the signal improves the performance of the discrimination but is not very practical as the scaling coefficient is determined after the fact. For the later YPG and APG Open Field demonstrations we employed another method to mitigate the effects of bouncing noise. Each target was fit using a full, unconstrained 3-β model as well as the library model. The ratio of the $\chi^2$ for these two methods, which eliminates the dependence on signal amplitude, should approach 1 if the item is in the library.

The ROC curves for the application of these three discrimination methods to the APG Blind Grid are shown in Figure A-5 through Figure A-7. The standard $\chi^2$ weighting (Figure A-5) and the modified weighting with "bounce noise" added (Figure A-6) result in curves that vary little from the chance diagonal. There are fewer items in Figure A-6 than in Figure A-5. The original submission to APG required that a discrimination score be included for all cells, even those below our detection threshold. We arbitrarily assigned these cells a low discrimination score. The $\chi^2$ with "bouncing noise" analysis was only applied to cells in which we declared a detection.

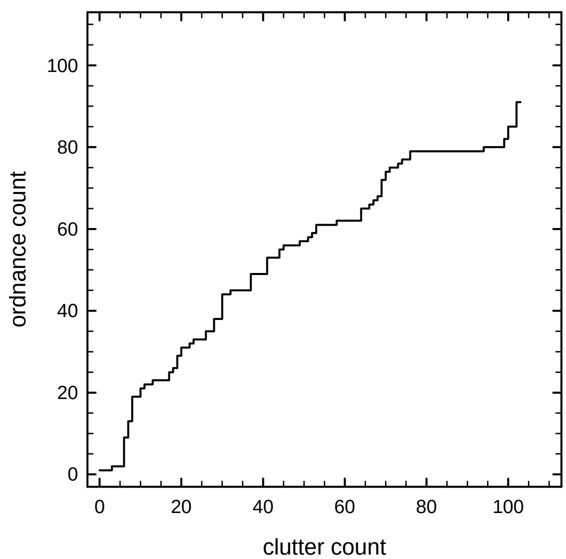


Figure A-5 – ROC curve for the $\chi^2$ weighting applied to the APG Blind Grid as shown in the left-hand side of Figures 25 and 26 of Reference 5

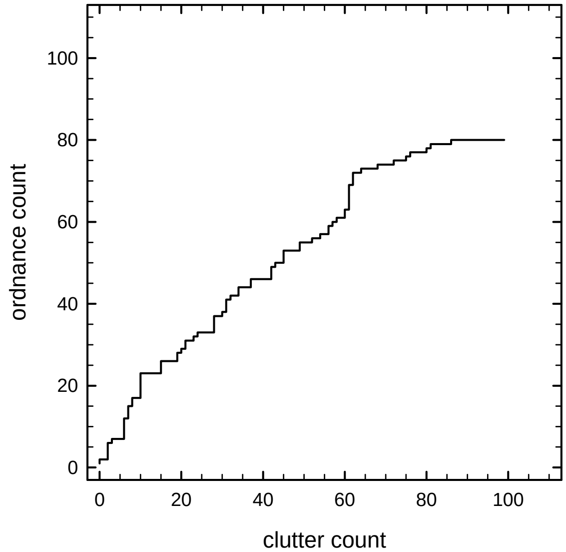


Figure A-6 – ROC curve for the case of $\chi^2$ weighting with an estimate of "bouncing noise" included applied to the APB Blind Grid

The $\chi^2$ ratio method (Figure A-7) does show some promise. Notice, however, that the curve in Figure A-7 includes even fewer ordnance and clutter items than in Figure A-6. The $\chi^2$ ratio method requires two different inversions to converge to sensible results in order to calculate the ratio. As the signal-to-noise ratio decreases, this becomes an increasingly difficult hurdle. Library methods such as this can work well when the expected targets are well defined but can provide inappropriate results when a munitions item not in the library is encountered.

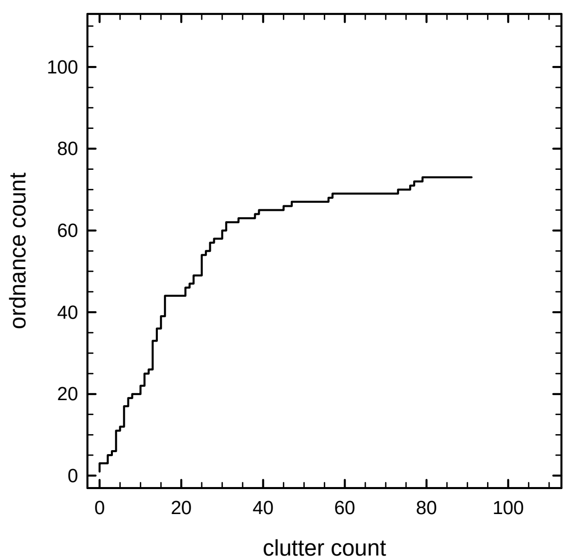


Figure A-7 – ROC curve for the $\chi^2$ ratio method applied to the APG Blind Grid

## A.2 Aberdeen Proving Ground Open Field

Selected results from our surveys at the Open Field at the Aberdeen Proving Ground Standardized Test Site have been provided to us by analysts at the Institute for Defense Analyses. These results are summarized graphically in the following sections.

### A.2.1 Response Stage

Response stage data from the Open Field scenario at the APG Standardized Test Site is shown in Figure A-8 as a plot of probability of detection vs. normalized background alarm rate. There are two analysis models shown on the plot. The first, the red line, corresponds to considering only those targets that were covered by the survey and are not within 2 m of another target. The analysis corresponding to the blue line retains those limitations and also excludes those targets deeper than 11x their diameter. We showed in Figure 20 of Reference 5 that the GEM array demonstrated is able to detect small and medium targets below this relative depth but our detection efficiency falls off at depths below 11x the item diameter. Response stage results broken out by item type are shown in Figure A-9. In this figure, the depth of 100% detection is denoted by the blue bar and the depth of maximum detection is shown as the horizontal line. For a number of the items, 105-mm HEAT for example, these two depths are the same. For the majority of the items, the maximum depth of detection is below the depth of 100% detection.

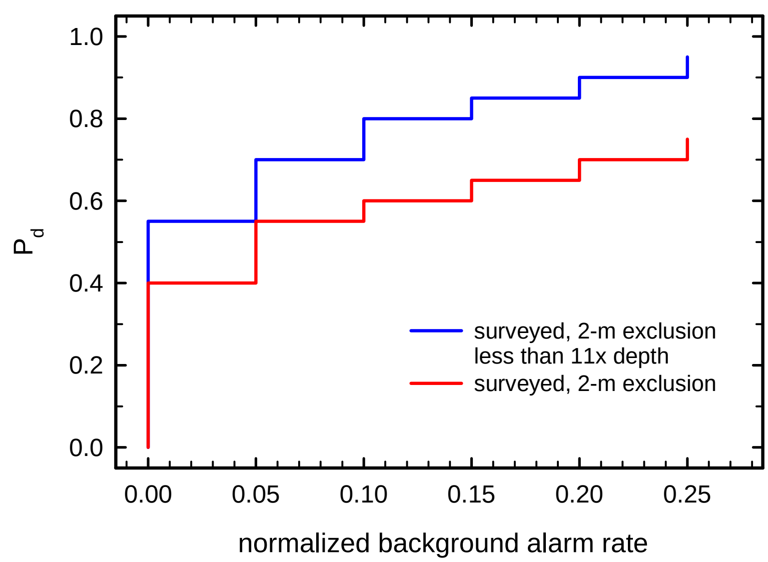


Figure A-8 – Detection performance at the APG Open Field Scenario. The red line is derived considering only targets that were covered in the survey and are not within 2 m of another target. The blue line retains those criteria and also excludes targets deeper than 11x their diameter.

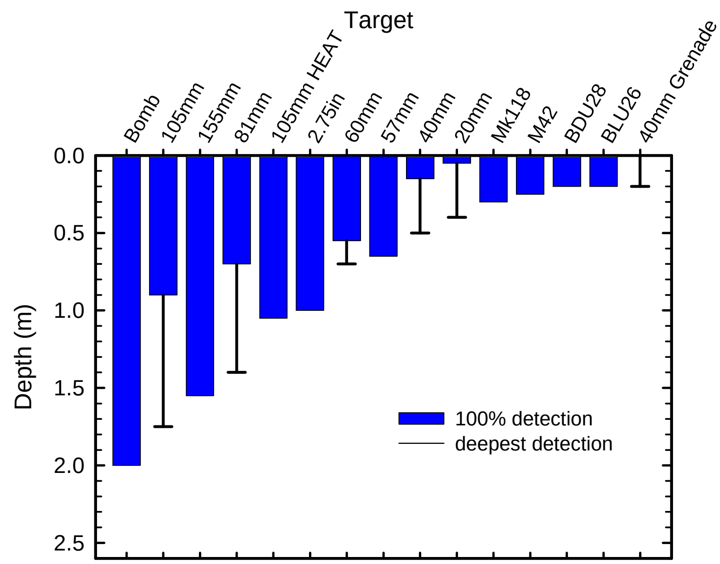


Figure A-9 – Response stage results for the APG Open Field scenario broken out by target type

### A.2.2 Discrimination Stage

Discrimination stage performance at the APG Open Field using the same two analysis models is shown in Figure A-10. As above, the exclusion of items at depths below 11x their diameter (presumably lower S/N anomalies) improves the discrimination performance obtained.

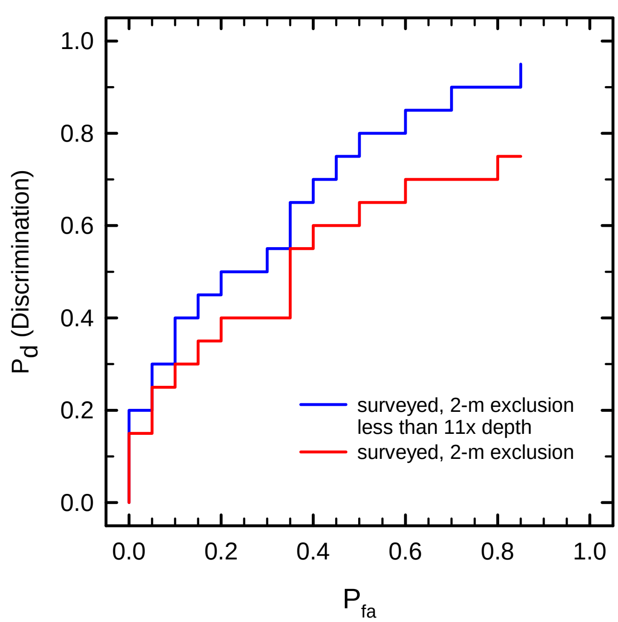


Figure A-10 – Discrimination performance at the APG Open Field Scenario. The red line is derived considering only targets that were covered in the survey and are not within 2 m of another target. The blue line retains those criteria and also excludes targets deeper than 11x their diameter.

### A.3 Yuma Proving Ground Open Field

Selected results from our surveys at the Open Field at the Yuma Proving Ground Standardized Test Site have been provided to us by analysts at the Institute for Defense Analyses. These results are summarized graphically in the following sections.

#### A.3.1 Response Stage

Response stage results for the YPG Open Field scenario are shown in Figure A-11 and Figure A-12. As for APG, they are analyzed by excluding first items that were not covered by the survey or are within 2-m of another item then retaining those exclusions and further excluding items deeper than 11x their diameter. Notice that the background alarm rates in Figure A-11 are more than a factor of two smaller than the corresponding results from Aberdeen. Although the Yuma site is more geologically active than Aberdeen, it is smoother so there were fewer false alarms due to platform bouncing over deep ruts. Detection depths at Yuma are, in general, in line with those obtained at Aberdeen. Note however, that a shallow bomb was apparently missed resulting in an unusual plot for that target type.

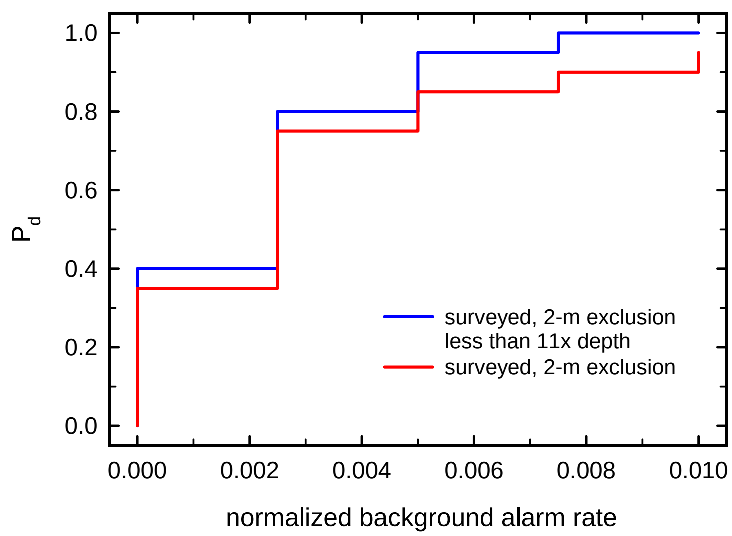


Figure A-11 – Detection performance at the YPG Open Field Scenario. The red line is derived considering only targets that were covered in the survey and are not within 2 m of another target. The blue line retains those criteria and also excludes targets deeper than 11x their diameter.

#### A.3.2 Discrimination Stage

Discrimination Stage results from the YPG Open Field are shown in Figure A-13. As before, exclusion of items that are deeper than 11x their diameter improves performance which is better, on the whole, than that observed at Aberdeen. As with the response stage, this is likely due to the lower platform motion noise observed at the Yuma site.

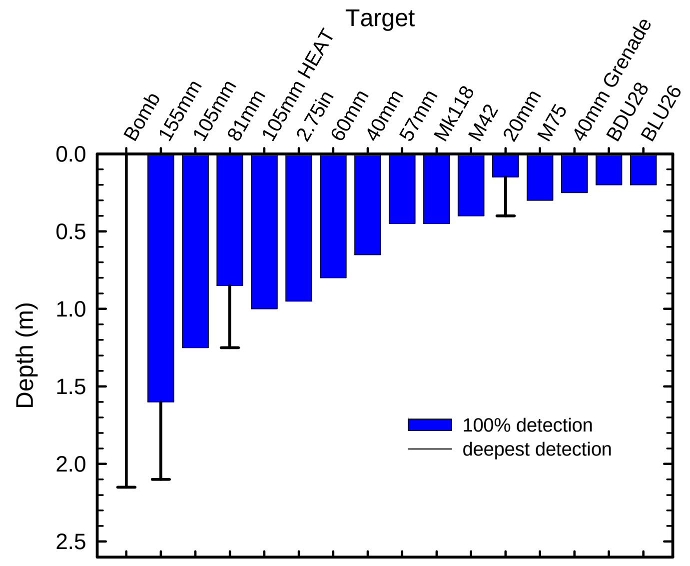


Figure A-12 – Response stage results for the YPG Open Field scenario broken out by target type

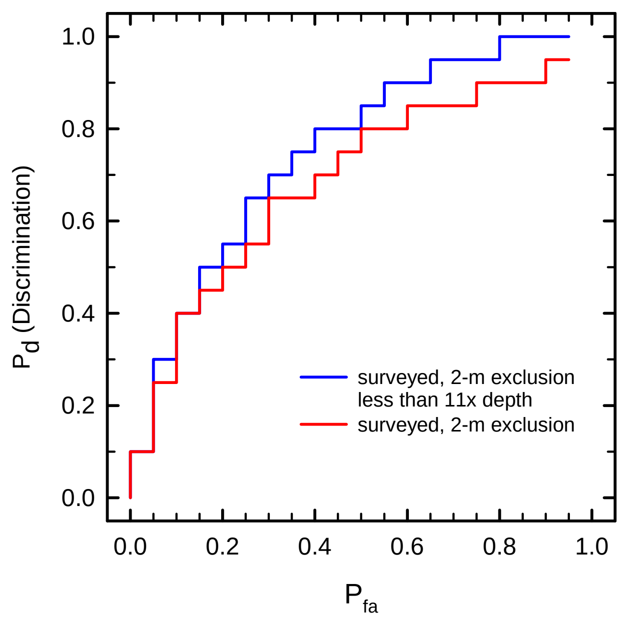


Figure A-13 – Discrimination performance at the YPG Open Field Scenario. The red line is derived considering only targets that were covered in the survey and are not within 2 m of another target. The blue line retains those criteria and also excludes targets deeper than 11x their diameter.

# Appendix B. Quality Assurance Project Plan (QAPP)

## B.1 Purpose and Scope of the Plan

The collection and archiving of high quality survey data in auditable and defensible manner is critical to insure the credibility of the data collected and to support decisions based in part or in total on that data. This Appendix outlines the standard process used in the NRL MTADS program to collect survey data, conduct quality checks to insure the quality of the data, and then process and archive the data. With the exception of Section B.9, the discussion focuses on the magnetometer array system. For the EM61 MkII and GEMTADS sensor systems similar procedures are used, different only in the details of the data collected for each sensor system. Any sensor platform unique items are indicated where appropriate.

## B.2 Quality Assurance Responsibilities

The team as a whole is involved in insuring the quality of collected data. The MTADS has been designed to provide a series of visual indicators to the operator regarding the status of the individual subsystems that comprise the MTADS. The operator is responsible for monitoring these indicators and halting data collection immediately if any problems are indicated. The issue will be resolved prior to resuming operations. All team members are involved in visual walk-around inspections of the system at least daily. For each survey file set, the data preprocessing tasks are logging receipt of the file set, archiving the file set, verifying that all files within the file set are valid, and verifying that each sensor channel contains valid data with sufficient SNR (where appropriate). Any section of data which is found lacking is flagged accordingly and not processed any further. The section will be logged for future re-acquisition if necessary. The data analyst is responsible for the data preprocessing and processing tasks with the site / project manager's assistance as available. Dr. Daniel Steinhurst will serve as the Quality Assurance Officer for this project.

## B.3 Data Quality Parameters

Incoming survey data will be evaluated for: completeness of the data set, location quality for the data set, and for proper operation of the magnetometer sensors. The following section details in an example how the data quality issues are addressed throughout the survey.

## B.4 Calibration Procedures, Quality Control Checks, and Corrective Action

The following procedure constitutes a typical startup for the MTADS system for both initial startup and as daily system evaluations. The RTK GPS base station receiver and radio link will be established on one of the established control points. The validity of the control point location will be verified using the MTADS man-portable RTK GPS rover receiver to occupy one or more of the established control points using the control point occupied by the GPS base station as a reference as required by the QAO.

For the GEMTADS array, the standard performance checks include three types of measurements. Initial system startup, at the beginning of field work and again each morning, consists of three measurements. First, quiet, static data are collected for a period (15 - 20 minutes or as directed by the QAO) with all systems powered up and warmed up (typically 30 minutes). Next, two calibration items, a 4" diameter Aluminum (Al) sphere and a ferrite rod bundle, are placed a standard distance above the center of each sensor coil several times in sequence to verify the response of each sensor to each object. The system is stationary for this data collection. Finally, a systems timing check using a fixed-position wire or chain placed on the ground is conducted. At the discretion of the QAO, the timing check may be repeated in the middle of the survey day. At the discretion of the QAO, the timing check and the Al sphere and ferrite measurements may be repeated at the end of the day. When all system checks are completed to the satisfaction of the QAO, the survey will commence.

For the EM61 MkII array, the standard performance checks are the same as for the GEMTADS with the ferrite rod measurements deleted. The ferrite rod is not a useful calibration item for this time-domain instrument. For the magnetometer array, the Al sphere measurements are also deleted and the quiet period is reduced to 5-10 minutes. Each sensor platform's performance check requirements are based on data rates and the historical stability and reproducibility of each sensor type.

Preventative maintenance inspections will be conducted at least once a day by all team members, focusing particularly on the tow vehicle and sensor trailer. Any deficiencies will be addressed according to the severity of the deficiency. Parts, tools, and materials for many maintenance scenarios are available in the system spares inventory which will be on site. Status on any break-downs / failures which will result in long-term delays in operations will be immediately reported to a representative of the Program Office.

MTADS survey raw data generally falls into two categories, location and sensor measurements. For the magnetometer array, the data set is comprised of ten separate files, each containing the data from a single system device. Each device has a unique data rate. A software package written by NRL examines each file and compares the number of entries to the product (total survey time * data rate). Any discrepancies are flagged for the data analyst to address. For magnetometer sensor data, operational values are typically on the order of 50,000 nT and have noise levels of ~0.5 nT peak-to-peak (PP) static and 3-5 nT PP in motion. Sensor "drop-outs" can occur if the sensor is tilted out of the operation zone with respect to the earth's magnetic field. If a sensor cable is severed or damaged while in motion, the sensor output value will drop below 20,000 nT and/or become very noisy (1,000's of nT PP). All magnetometer sensor channels (8 total) are examined in each survey file set for these conditions and any data which is deemed unsatisfactory is flagged and not processed further. For location data, the RTK GPS receivers present a Fix Quality value that relates to the quality / precision of the reported position. A Fix Quality (FQ) value of 3 (RTK Fixed) is the best accuracy (typically 3-5 cm or better). A FQ value of 2 (RTK Float) indicates that the highest level of RTK has not be reached yet and location accuracy can be degraded to as poor as ~1 m. FQ 1 & 4 correspond to Autonomous and DGPS operational modes respectively. Data collected under FQ 3 and FQ 2 (at the discretion of the data analyst) are retained. Any other data are deemed unsatisfactory, flagged and not processed further. The survey section containing the flagged data will be logged for future re-acquisition if required. Data which meet these standards are of the quality typical of the MTADS system.

For the EM61 MkII array, stationary sensor noise levels were approximately 1 mV for all time gates at the Former Camp Sibert ESTCP UXO Discrimination Study demonstration [7] and the dynamic background signal levels on the calibration lane were 1.6 ± 0.1 mV, s1. The corresponding GEMTADS results were 0.232 ± 0.177 ppm, $Q_{ave}$ for stationary measurements and the dynamic background level was 0.35 ± 0.06, $Q_{ave}$ for the calibration lane. Also note that for the EM61 MkII and GEMTADS arrays, the orientation of the platform is also recorded as described in Section 2. Two additional GPS strings of the "PTNL, AVR" type are recorded and the output of the IMU is also recorded. Similar quality checks are applied to these additional data sources.

## B.5 Demonstration Procedures

See Section B.4. The same discussion applies to this section.

## B.6 Calculation of Data Quality Indicators

There are no specialized equations required. The methods are outlined in Section B.4.

## B.7 Performance and System Audits

See Section B.4. The same discussion applies to this section.

## B.8 Quality Assurance Reports

The results of the daily system checkout runs for the standard systems checks and the dynamic survey of the emplaced items will be reported to the QAO daily. The Data Analyst will report any data sections requiring reacquisition to the site / project manager for a given day by the start of work the following morning.

## B.9 GEM-3 (GEMTADS) Array Data File Formats

Each survey file set contains eight files which constitute the 'raw data'. The file name structure is based on the date and time of the start logging event (MMMDDYYYY_HHMMSS). Data in each file is time stamped with the appropriate clock to allow synchronization between files.

**MMMDDYYYY_HHMMSS.Survey.AVR1.csv**
GPS output, Trimble PTNL,GGK sentence at 20 Hz (position), PTNL,AVR sentence for MB1 / MB2 receiver pair at 10 Hz (orientation).
**MMMDDYYYY_HHMMSS.Survey.AVR2.csv**
GPS output, Trimble PTNL,AVR sentence for MB2 / MR receiver pair at 10 Hz (orientation).
**MMMDDYYYY_HHMMSS_ID1.Survey.GEM.csv**
Output from Sensor #1 (Port, Forward), In-phase and Quadrature data for 9 frequencies.
**MMMDDYYYY_HHMMSS_ID2.Survey.GEM.csv**
Output from Sensor #2 (Center, Aft), In-phase and Quadrature data for 9 frequencies.
**MMMDDYYYY_HHMMSS_ID3.Survey.GEM.csv**
Output from Sensor #3 (Starboard, Forward), In-phase and Quadrature data for 9 frequencies.
**MMMDDYYYY_HHMMSS.Survey.PPS.csv**
pulse per second (PPS) from GPS receiver, 1 Hz.
**MMMDDYYYY_HHMMSS.Survey.IMU.tbf**

```
      Output from IMU (pitch, roll, angular rates, accelerations, etc.) in packed
      binary format.
MMMDDYYYY_HHMMSS.Survey.UTC.csv
      UTC time tag from GPS receiver MR, "The time will be" message for next PPS, 1
      Hz.
```

The IMU data are recorded in a packed binary data format with a time tag appended periodically. The data packet format is described in the manufacturer's manuals and technical notes and is not reproduced here. The GEM-3 data files are well annotated internally and the format is not discussed here.

Located data archives are stored in an ASCII file format of the form:

For located, demedianed GEM-3 data:

```
T            UTC time in seconds past midnight
X            (UTM Zone X, NAD83, m) Easting for GPS antenna
Y            (UTM Zone X, NAD83, m) Northing for GPS antenna
Z            (WGS84, m) Height above Ellipsoid for GPS antenna
COG          (degrees) Course over ground (Heading) of array in Grid North
              frame, North = 0 degrees
GPS_Roll     (degrees) Roll of the sensor platform from GPS array
GPS_Pitch    (degrees) Pitch of the sensor platform from GPS array
IMU_Roll     (degrees) Roll of the sensor platform from IMU
IMU_Pitch    (degrees) Pitch of the sensor platform from IMU
SensorID     Denotes which sensor data are from
I_90Hz       (ppm) Demedianed GEM-3 data for 90 Hz, In-phase Response
Q_90Hz       (ppm) Demedianed GEM-3 data for 90 Hz, Quadrature Response
...

I_20010Hz    (ppm) Demedianed GEM-3 data for 20,010 Hz, In-phase Response
Q_20010Hz    (ppm) Demedianed GEM-3 data for 20,010 Hz, Quadrature Response
Filename     Filename of source data file
```

where X is the appropriate UTM zone (13N for Cheyenne, WY)

### B.10 Data Storage and Archiving Procedures

Data are stored electronically as collected on the MTADS vehicle DAS computer hard drive. Approximately every two survey hours, the collected data are copied onto magnetic disks (Iomega ZIP 250) or removable media and transferred to the data analyst. The data are moved onto the data analyst's computer and the media is recycled. Raw data and analysis results are backed up from the data analyst's computer to optical media (CD-R or DVD-R) or external hard disks daily. These results are archived on an internal file server at NRL at the end of the survey. All field notes / activity logs are written in ink and stored in archival laboratory notebooks. These notebooks are archived at NRL or SAIC. Relevant sections are reproduced in demonstration reports. Dr. Daniel Steinhurst is the POC for obtaining data and other information. His contact information is provided in Section 5 of this report.